

# UC San Diego

## UC San Diego Electronic Theses and Dissertations

### Title

Amyloid precursor protein and axonal transport

### Permalink

<https://escholarship.org/uc/item/38n9j13r>

### Author

Rodrigues, Elizabeth M.

### Publication Date

2010

Peer reviewed|Thesis/dissertation

UNIVERSITY OF CALIFORNIA, SAN DIEGO

Amyloid precursor protein and axonal transport

A dissertation submitted in partial satisfaction of the requirements for the degree  
Doctor of Philosophy

in

Neurosciences

by

Elizabeth M. Rodrigues

Committee in charge:

Professor Lawrence Goldstein, Chair  
Professor Laura Dugan  
Professor Edward Koo  
Professor Eliezer Masliah  
Professor David Williams

2010

©

Elizabeth M. Rodrigues, 2010

All rights reserved.

The Dissertation of Elizabeth M. Rodrigues is approved, and it is acceptable in quality and form for publication on microfilm and electronically:

---

---

---

---

---

---

Chair

University of California, San Diego

2010

## TABLE OF CONTENTS

Signature page .....	iii
Table of Contents .....	iv
List of figures .....	v
Acknowledgements .....	vii
Curriculum Vitae .....	ix
Abstract .....	xv
Chapter I – Amyloid precursor protein and its relationship to axonal transport .	1
Chapter II – Mutations at the $\beta$ -secretase cleavage site of APP mediates its axonal transport .....	10
Abstract .....	11
Introduction .....	12
Methods .....	15
Results .....	21
Discussion .....	31
Chapter III – Axonal defects in an FAD Swedish mutant APP gene-targeted mouse .....	53
Abstract .....	54
Introduction .....	55
Methods .....	58
Results .....	63
Discussion .....	68
Chapter IV – Conclusions .....	79
References .....	83

## LIST OF FIGURES

Figure 1.1.	Cleavage pathways of APP .....	9
Figure 2.1.	APP-YFP and mutations .....	40
Figure 2.2.	Mutations of APP-YFP that alter $\beta$ -secretase cleavage .....	41
Figure 2.3.	Mutant APP-YFP undergoes axonal transport .....	42
Figure 2.4.	Effect of Swedish mutations on percentages of APP-YFP movement .....	43
Figure 2.5.	Effect of Swedish mutations on segmental velocities and segmental run lengths .....	44
Figure 2.6.	Effect of $\beta$ -secretase inhibitor on percentages of Swedish APP-YFP movement .....	45
Figure 2.7.	Effect of $\gamma$ -secretase inhibitor on percentages of Swedish APP-YFP movement .....	46
Figure 2.8.	Effect of MV mutation on percentages of APP-YFP movement ...	47
Figure 2.9.	Effect of MV mutation on segmental velocities and segmental run lengths .....	48
Figure 2.10.	Effect of $\beta$ -secretase inhibitor on percentages of MV APP-YFP movement .....	49
Figure 2.11.	Effect of mutations on axonal APP-YFP vesicle number and fluorescence intensity .....	50
Figure 2.12.	Opposite effects of Swedish and MV mutations on percentages of movement .....	51
Figure 2.13.	MV mutation specifically affects anterograde segmental velocity and segmental run length .....	52

Figure 3.1.	Gene-targeted mutations in the mouse APP gene .....	72
Figure 3.2.	Backcrossed gene-targeted mice express humanized APP .....	73
Figure 3.3.	Axonal dilation in the septo-hippocampal subregion of the septal nucleus .....	74
Figure 3.4.	No axonal dilation in other subregions of the septal nucleus .....	75
Figure 3.5.	No hippocampal terminal field changes in the inner molecular layer of the dentate gyrus .....	76
Figure 3.6.	No presynaptic bouton density changes in other hippocampal terminal field regions examined .....	77
Figure 3.7.	No axonal swellings in the NBM of J20 mice .....	78

## ACKNOWLEDGEMENTS

I would like to thank Dr. Larry Goldstein for letting me do this thesis work in his laboratory. Without his support, this project could not have been done. My thesis committee also provided valuable guidance. Their time and energy is greatly appreciated. Particularly, I would like to thank Dr. Edward Koo for providing J20 transgenic APP mice used in a collaborative project. Dr. Eliezer Masliah also provided human brain tissue used in another study. The members of the Goldstein lab have provided immeasurable scientific and moral support. Their mentorship and counseling were crucial during my time in graduate school and the Goldstein lab, and I am forever thankful to them. In particular, I would like to thank Dr. Lu-Shiun Her, Dr. Jason Duncan, Dr. Angels Almenar, Jessica Flippin, and Emily Niederst.

My work was supported primarily by an individual predoctoral Ruth L. Kirschstein National Research Service Award (Fellowship #5F31AG027688). Additional support was provided by Dr. Larry Goldstein, the Neuroscience Graduate Program, National Institutes of Health Scholars Program, and Merck Pharmaceuticals.



Chapters II and III are currently being prepared for submission and publication of the material. Rodrigues EM and Goldstein LSB. The dissertation author was the primary author and investigator of this paper.

## CURRICULUM VITAE

### Education

- 2010 Ph.D. in Neuroscience, University of California at San Diego  
Thesis Advisor: Dr. Lawrence Goldstein, Howard Hughes  
Medical Investigator, Cellular and Molecular Medicine
- 2001 B.S., B.A. in Biology, Robert D. Clarke Honors College,  
University of Oregon, Eugene, OR  
Thesis Advisor: Dr. Janis Weeks, Institute of Neuroscience
- 1997 High school diploma  
St. Mary's Academy, Portland, OR

### Research Experience

- 2004 –2010 Graduate student, University of California at San Diego. La Jolla, CA.  
Laboratory of Dr. Lawrence Goldstein  
Invested the involvement of amyloid precursor protein (APP) and axonal transport defects in Alzheimer's disease (AD) pathogenesis. Showed that familial AD Swedish mutations to APP 1) impair APP axonal transport and 2) are sufficient to lead to axonal dystrophy in the absence of amyloid plaques.
- 2001-2003 Research technician, Institute of Neuroscience, University of Oregon.  
Eugene, OR. Laboratory of Dr. Janis Weeks.  
Studied mitochondrial events in neuronal death of the hawk moth, *Manduca sexta*. Showed that motoneurons undergoing steroid-induced, autophagic programmed cell start to lose their mitochondrial transinnermembrane potential early in the death pathway and before mitochondria aggregate.
- 2001 Head Course Assistant, *Neural Systems and Behavior*, Marine Biological Laboratory. Woods Hole, MA.  
Helped organize lectures and execute laboratory experiments. Oversaw course administrative details. Assisted in dissections and

fluorescent microscopy. Prepared and ordered laboratory materials and solutions.

2000-2001 Undergraduate senior thesis research, Institute of Neuroscience, Robert D. Clarke Honors College, University of Oregon. Eugene, OR. Laboratory of Dr. Janis Weeks.

Studied neuronal cell death in the hawk moth. Used the TUNEL assay, an assay for DNA fragmentation previously thought to be diagnostic of apoptotic programmed cell death, to show that motoneurons dying by autophagic programmed cell death also undergo DNA fragmentation.

1998-2000 Summer and Winter Internships, Kaiser Permanente Center for Health Research. Portland, OR.

Researched the efficacy of the triple maternal serum prenatal test in successfully predicting birth and chromosomal abnormalities of newborns. Studied the impact a breast cancer educational computer program had on women and their decisions regarding breast cancer health.

1996-1997 Summer and Winter Internships, Oregon Health Sciences University, Department of Neuroscience. Portland, OR. Laboratory of Dr. Martha Neuringer.

Showed behavioral differences between rhesus monkeys fed diets either high or low in omega-6 fatty acid levels. Omega-6 essential fatty acids, high in a mother's breast milk but deficient in baby formulas, play important roles in cognitive and eye development.

### Publications

Falzone TL, Stokin GB, Lillo C, Rodrigues EM, Westerman EL, Williams DS, Goldstein LSB. 2009. Axonal stress kinase activation and tau misbehavior induced by kinesin-1 transport defects. *J Neurosci.*, 29:5758-67.

Stokin GB, Almenar-Queralt A, Gunawardena S, Rodrigues EM, Falzone T, Kim J, Lillo C, Mount SL, Roberts EA, McGowan E, Williams DS, Goldstein LSB. 2008.

Amyloid precursor protein-induced axonopathies are independent of amyloid-beta peptides. *Hum Mol Genet.* 17:3474-86.

Kinch G, Hoffman KL, Rodrigues EM, Zee MC, Weeks JC. 2003. Steroid-triggered programmed cell death of a motoneuron occurs by autophagy and involves structural changes in mitochondria. *J. Comp. Neurol.*, 457: 384-403.

Rodrigues EM, Bucknell-Pogue T, Thorkildson JA, Rutherford MA, Weeks JC. In progress. Mitochondrial dysfunction during the steroid-induced programmed cell death of a motoneuron.

### Abstracts

Rodrigues EM, Goldstein LSB. 2009. Altered axonal transport of  $\beta$ -secretase cleavage site mutant amyloid precursor protein. Program No. 428.2. Abstract Viewer/Itinerary Planner. Washington, DC: Society for Neuroscience. Online.

Rodrigues EM, Price DL, MacLean NAB, Martone ME, Bash R, Van Dyke T, Ellisman MH. 2004. Diffusely transformed astrocytes by sv40 expression as a model for brain cancer: alterations in filamentous-actin levels. Program No. 462.12. Abstract Viewer/Itinerary Planner. Washington, DC: Society for Neuroscience. Online.

M.A. Rutherford, T. Bucknell-Pogue, E.M. Rodrigues, and J.C. Weeks. 2002. Mitochondrial events during the steroid-mediated programmed cell death of motoneurons. Program No. 31.3. Abstract Viewer/Itinerary Planner. Washington, DC: Society for Neuroscience. Online.

### Awards and Fellowships

- |           |   |
|-----------|---|
| 2006-2010 | Individual Predoctoral NRSA, National Institute on Aging, National Institutes of Health, F31 AG027688 |
| 2005-2006 | Neuroplasticity in Aging Training Grant   |
| 2004-2005 | Merck Industries Fellowship   |
| 2003-2004 | NIH Scholars Program  |

- 2000-2003 Ronald E. McNair Scholars Program
- 2001 Robert D. Clarke Honors College and Department of Biology Honors Undergraduate Thesis with Distinction Award
- 2000 Summer Program in Undergraduate Research, University of Oregon and the National Science Foundation's IGERT grant
- 1997-2001 Underrepresented Minority Achievement Scholarship
- 1997 Bonneville Power Administration Minority Scholarship
- 1996-1997 Apprenticeships in Science and Engineering

Scientific Presentations and Meetings

- 2002, 2004, 2007, 2009 Society for Neuroscience Poster Presentations
- 2001- 2010 Society for Neuroscience
- 2001 University of Oregon's Robert D. Clark Honors College and Department of Biology Honors Thesis Defense, May 24. Eugene, OR
- 2000 University of Oregon's McNair Scholars Program Symposium, August 12. Eugene, OR
- 2000 University of Oregon's Summer Program for Undergraduate Research, August 4. Eugene, OR
- 2001 IGERT Symposium, The Evolution of Genetic Networks, October 12-14. Eugene, OR
- 1998 Kaiser Permanente Center for Health Research Internship Presentation, August. Portland, OR

- 1996, 1997 Oregon Regional Primate Research Center Annual Internship Symposium, August. Portland, OR
- 1996, 1997 Apprenticeships in Science and Engineering Annual Symposium, August. Portland, OR

### Teaching Experience

- 2009-2010 Mentor, undergraduate research project, University of California, San Diego
- 2004, Fall Teaching assistant, Human Development Program 101
- 2001-2003 Co-mentor, Department of Biology and Honors College undergraduate thesis, University of Oregon. Eugene, OR
- 2001 Presentation and laboratory tour, "How steroid hormones orchestrate changes in development and behavior: the moth *Manduca sexta* as a model system," Sophomore psychology class, North Eugene High School. Eugene, OR
- 2000 Presentation and laboratory tour, "Steroid control of metamorphosis in the moth *Manduca sexta*," Summer High School Apprenticeship Program, Institute of Neuroscience, University of Oregon. Funded through NCRR K-12 Summer Program, NIH. Eugene, OR
- 1998-1999 Co-coordinator for teen social health workshop, African American Wellness Village. Portland, OR
- 1995-1996 Student science instructor and youth leader for Oregon public school system's Outdoor Education Program. Multnomah County, Oregon

### Technical Training and Skills

- 2004 Stereology Course, Peter R. Mouton. San Diego, October 20-23.

- 2004 Light and Electron Microscopy Techniques Course, University of California at San Diego. Spring.
- 2002 Confocal and Multiphoton Workshop, University of Oregon. December 5-6.
- 2001 Electron Microscopy Course, University of Oregon. Winter.

ABSTRACT OF THE DISSERTATION

Amyloid precursor protein and axonal transport

by

Elizabeth M. Rodrigues

Doctor of Philosophy in Neurosciences

University of California, San Diego, 2010

Professor Lawrence Goldstein, Chair

Amyloid precursor protein (APP) is intimately involved in the pathogenesis of Alzheimer's disease (AD), a neurodegenerative disease characterized by cognitive decline, amyloid plaques, and neurofibrillary tangles. Beta-secretase cleavage of APP is the first step in the amyloidogenic cleavage pathway that is enhanced in AD and generates amyloid beta peptides, the primary component of amyloid plaques. It is not clear how this enhanced amyloidogenic cleavage of APP can lead to AD pathology, but research has



indicated that defects in axonal transport may contribute to disease progression. Signs of axonal transport defects develop in AD and animal models of amyloid pathology well before amyloid plaques deposit. It remains unknown how increased beta-secretase cleavage affects APP axonal transport and can lead to axonal defects.

This thesis project shows that enhanced beta-secretase cleavage of APP impairs APP axonal transport *in vitro* and leads to axonal dystrophy *in vivo*, suggesting that disrupted axonal transport of APP might contribute to disease pathogenesis. First, I used a fluorescently-tagged version of the APP protein to show that 1) the familial AD (FAD) Swedish mutations at the beta-secretase cleavage site of APP increase beta-secretase cleavage and inhibit APP anterograde axonal transport, and 2) an opposing mutation at the beta-secretase cleavage site decreases beta-secretase cleavage and enhances APP anterograde axonal transport. Next, I used a gene-targeted mouse model to show that 1) FAD Swedish mutant APP expressed at endogenous levels can lead to axonal dilation in the cholinergic basal forebrain, and 2) axonal dystrophy develops in the absence of amyloid plaques. Taken together, these data suggest that amyloidogenic cleavage of APP, which is enhanced in AD, disrupts APP axonal

transport and leads to axonal dystrophy before amyloid plaque formation, presenting a possible mechanism contributing to AD pathogenesis.

Chapter I -

AMYLOID PRECURSOR PROTEIN AND ITS RELATIONSHIP TO AXONAL  
TRANSPORT

## **Introduction**

Alzheimer's disease (AD) is a neurodegenerative disease involving axonal transport defects, but precise mechanisms underlying these transport defects remain unknown. Aberrant processing of amyloid precursor protein (APP) plays an integral role in AD pathogenesis, which poses an intriguing possibility that disrupted axonal transport of APP itself could underlie axonal defects observed in AD.

### **Alzheimer's disease and axonal transport**

AD is a prevalent and progressive neurodegenerative disease characterized by cognitive decline and memory loss. The brains of AD patients characteristically develop extracellular amyloid plaques and intraneuronal neurofibrillary tangles. Amyloid plaques are insoluble aggregates consisting primarily of amyloid  $\beta$  peptides ( $A\beta$ ) that result from proteolytic cleavage of APP. Neurofibrillary tangles consist of paired helical filaments that form upon abnormal phosphorylation of the protein tau. AD pathology also includes dystrophic neurites, synaptic loss, and neuronal loss.

Axonal defects are a part of disease pathology, and some of these axonal changes are associated with plaques and tangles. White matter, the brain region consisting primarily of axons, is reduced in size in AD brains, and amyloid

plaques can deposit there. (Uchihara *et al.* 1995) Dystrophic neurites are prevalent in AD brains, particularly surrounding amyloid plaques. These abnormal neurites are often dilated and can stain for tau and/or neurofilaments. Tau is a microtubule-associated protein important for microtubule assembly and stabilization and neurite outgrowth. (Friedhoff *et al.* 2000) Microtubules are cytoskeletal components that help provide structure and serve as highways for axonal transport. Neurofibrillary tangles form upon abnormal phosphorylation of the microtubule-associated protein tau.

Although amyloid plaques and neurofibrillary tangles are diagnostic criteria for AD, it has become apparent that brain cells are already too sick to function properly by the time they develop; thus, investigating the events that precede plaques and tangles is crucial. Previous work in the Goldstein lab has identified an axonal defect in AD that develops before plaque or tangle formation, and this defect is one of disrupted axonal transport.

Axonal transport is a fundamental process necessary for neuronal function and signaling. Material synthesized in the cell body must reach the distantly-located synapse, plus other signaling must occur from the synapse to the cell body. This happens through a process called axonal transport. During axonal transport, material is packaged in membrane-bound vesicles that attach to

motor proteins. Motor proteins carry these cargo vesicles long distances along microtubule tracks within the axon to terminal destinations. The motor protein kinesin carries cargo in the anterograde direction away from the cell body and towards the synapse, while the motor protein dynein carries cargo in the retrograde direction towards the cell body.

Axonal transport defects play a role in AD pathogenesis prior to plaque or tangle formation. Sporadic AD brains develop axonal swellings (Stokin *et al.* 2005), an indicator of axonal transport defects that was previously characterized in animal models with deleted or mutated motor proteins. (Hurd and Saxton, 1996) Axonal swellings consist of accumulated vesicles and organelles. Such axonal accumulations could prevent normal delivery of necessary material to synapses and disrupt proper signaling, representing an early contributory event in disease pathogenesis. Other research further supports the contribution of axonal transport defects in AD. One study reports that a polymorphism of the gene encoding for the kinesin I motor protein subunit kinesin light chain 1 (KLC1) is significantly associated with AD. (Dhaenens *et al.* 2004) Another study demonstrates defective axonal transport in the temporal cortex of AD brains. (Dai *et al.* 2002)

Motor protein dysfunction and defects in axonal transport are related to other neurodegenerative diseases besides AD. Kinesin mutations are associated with Charcot-Marie Tooth disease and hereditary spastic paraplegia, and dynein mutations are associated with motor neuron degeneration. (Roy *et al.* 2005; LaMonte *et al.* 2002; Zhao *et al.* 2001; Reid *et al.* 2002; Puls *et al.* 2003) Because kinesin and dynein motor proteins have essential roles in neuronal biology, they can play crucial roles in neurodegenerative pathways. (Goldstein 2003; Cavalli *et al.* 2005; Stokin *et al.* 2005)

### **Amyloid precursor protein, AD, and axonal transport**

The vast majority of AD cases are sporadic, meaning there is no known genetic link. The small percentage of familial AD (FAD), or genetically-linked, cases identifies genetic mutations in APP or proteolytic processing component presenilin (PS1 and PS2). The full-length, transmembrane APP protein can be cleaved into a variety of fragments by a combination of either an  $\alpha$ - or a  $\beta$ -secretase and a  $\gamma$ -secretase. (Figure 1.1) APP cleavage happens all the time and serves important signaling functions.  $\beta$ -secretase cleavage, however, is particularly important to understand, as it can lead to disease. If full-length APP is first cleaved by  $\beta$ -secretase, APP enters the amyloidogenic cleavage pathway. In the amyloidogenic pathway,  $\beta$ -secretase cleavage of APP generates a C-

terminal fragment of APP (CTF) that is subsequently cleaved by  $\gamma$ -secretase to generate a soluble A $\beta$  peptide. A $\beta$  peptides aggregate as the primary component of the amyloid plaques that characterize AD. In sporadic AD, the amyloidogenic pathway is enhanced, and there is an increased level of A $\beta$  and amyloid plaque deposition. FAD mutations to APP or presenilin also enhance amyloidogenic proteolytic processing of APP to increase A $\beta$  generation, or the ratio of the 42 to 40 amino acid long A $\beta$  variants, and lead to plaque deposition. (Suzuki *et al.* 1994; Scheuner *et al.* 1996)

APP proteolytic processing plays an essential role in AD pathogenesis, and it has an important role in axonal transport. Not only does APP undergo axonal transport, but aberrant proteolytic processing of APP leads to signs of axonal transport defects. Research indicates that APP undergoes fast anterograde axonal transport via kinesin I motor protein. (Koo *et al.* 1990; Sisodia *et al.*, 1993; Kamal *et al.* 2001) FAD mutations to APP lead to signs of axonal transport defects. The FAD Swedish mutations to APP consist of two amino acid changes immediately adjacent to the  $\beta$ -secretase cleavage site of APP that enhance the  $\beta$ -secretase-dependent amyloidogenic cleavage pathway. A transgenic mouse model of AD amyloid pathology that overexpresses FAD Swedish mutant human APP under the prion promoter (TgAPP<sup>Swe</sup>) develops signs of axonal



transport defects. (Stokin *et al.* 2005) Axonal swellings form in cholinergic axons of the basal forebrain well before amyloid plaques deposit. These axonal swellings are directly relevant to AD pathology; they also develop in basal forebrain cholinergic axons of sporadic AD brains, which also undergo aberrant APP processing.

Axonal transport, particularly of APP, may contribute to AD pathological progression. Dystrophic neurites and cytoskeletal pathology in AD suggest axonal transport failure in disease progression. (Wisniewski *et al.* 1976; Masliah *et al.* 1990; Crowther and Goedert 2000) Because axonal swellings develop well before amyloid plaques deposit, axonal transport defects could be an early contributory event. Axonal injury causes APP and fragments, including A $\beta$ , to accumulate. (Kawarabayashi *et al.* 1993; Smith *et al.* 2003) Plus, TgAPP<sup>Swe</sup> mice with reduced motor protein subunit KLC1 have increased axonal swellings, A $\beta$ , and plaques. (Stokin *et al.* 2005) Thus, an assault to axonal health, such as defective axonal transport, might further contribute to aberrant APP processing. Furthermore, axonal transport of APP appears to be necessary for amyloid plaque formation. In a mouse model of amyloid pathology, plaque formation was inhibited in the hippocampus when axons projecting to this region were severed. (Lazarov *et al.* 2002; Sheng *et al.* 2002)

## Thesis research

AD brains exhibit aberrant APP processing and axonal transport defects, plus FAD mutant APP that causes aberrant processing can lead to axonal transport defects. Despite this connection between AD and APP and axonal transport defects, it remains unclear if axonal transport of APP is altered in AD and what mechanisms might underlie the axonal defects observed. Research conducted in this thesis project tested the hypotheses that the FAD Swedish mutations to APP can cause disrupted axonal transport of APP *in vitro* and are sufficient to lead to axonal dystrophy *in vivo*. Such findings would suggest that aberrant processing of APP disrupts its axonal transport and could contribute to the axonal dystrophy that develops in AD. The FAD Swedish mutations are located at the  $\beta$ -secretase cleavage site of APP, and  $\beta$ -secretase cleavage is the first step of the amyloidogenic cleavage pathway that generates  $A\beta$  and is enhanced in AD. The FAD Swedish mutations to APP have previously been demonstrated to lead to axonal swellings, a morphological indicator of disrupted axonal transport.

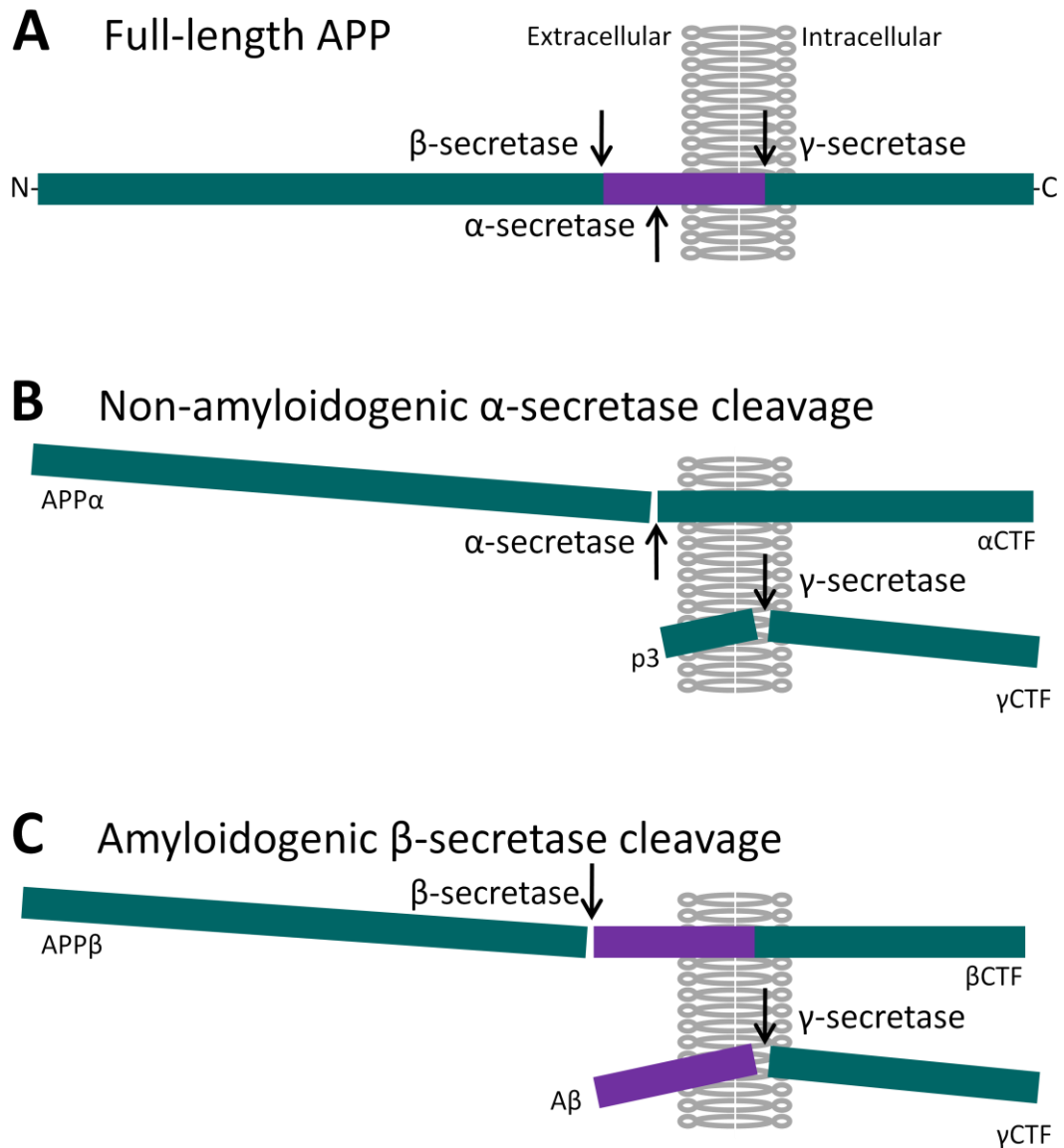


Figure 1.1. Cleavage pathways of APP. A) Full-length APP is a transmembrane protein that can be cleaved by  $\alpha$ -,  $\beta$ -, and  $\gamma$ -secretases. B) The non-amyloidogenic cleavage pathway begins with  $\alpha$ -secretase cleavage, which generates a soluble APP $\alpha$  fragment. The remaining  $\alpha$ CTF fragment is subsequently cleaved by  $\gamma$ -secretase to create  $\gamma$ CTF and p3 fragments. C) The amyloidogenic cleavage pathway begins with  $\beta$ -secretase cleavage, which generates a soluble APP $\beta$  fragment. The remaining  $\beta$ CTF fragment is subsequently cleaved by  $\gamma$ -secretase to create  $\gamma$ CTF and A $\beta$  fragments. These A $\beta$  peptides (shown in purple) are the primary component of the amyloid plaques that characterize AD.

Chapter II -  
MUTATIONS AT THE  $\beta$ -SECRETASE CLEAVAGE SITE OF APP MEDIATE ITS  
AXONAL TRANSPORT

**Abstract**

Brains of sporadic AD patients and TgAPP<sup>Swe</sup> mice develop axonal swellings, an indicator of disrupted axonal transport, well before the amyloid plaques that characterize the disease. (Stokin *et al.* 2005) Increased  $\beta$ -secretase cleavage of APP occurs in sporadic AD and results from the FAD Swedish mutations to APP, but its effect on axonal transport of APP remains unknown. Research described in this chapter demonstrates that the FAD Swedish mutations at the  $\beta$ -secretase cleavage site of a fluorescently-tagged version of APP impair anterograde axonal transport of the protein. This phenotype can be reversed with a  $\beta$ -secretase inhibitor and exacerbated with a  $\gamma$ -secretase inhibitor. Conversely, an opposing mutation at the same  $\beta$ -secretase cleavage site of APP, which inhibits  $\beta$ -secretase cleavage of APP, has the opposite effect by promoting anterograde axonal transport. These data suggest that  $\beta$ -secretase cleavage of APP mediates its axonal transport and suggest that axonal defects that develop upon aberrant APP processing could possibly develop through disrupted axonal transport of APP.

## Introduction

AD pathogenesis includes aberrant APP processing and axonal transport defects, and APP disruptions lead to axonal transport defects. This prompts the question if aberrant APP processing is able to impair axonal transport of APP itself. If this were the case, it suggests an intriguing possibility that APP processing changes that occur in AD could lead to the axonal transport defects observed in the disease.

A wealth of data supports that disruptions in APP impair axonal transport. For example, TgAPP<sup>Swe</sup> mice that overexpress FAD Swedish mutant APP and undergo aberrant APP processing exhibit axonal transport defects. They develop axonal swellings, a phenotype of disrupted axonal transport, well before plaques deposit. (Stokin *et al.* 2005) These mice also demonstrate defective retrograde transport of neural growth factor (NGF). (Salehi *et al.* 2006) Additionally, overexpressed FAD mutant PS1, which also influences APP processing and A $\beta$  generation (Kim *et al.* 2001; Leem *et al.* 2002), may reduce APP trafficking to terminal destinations. (Cai *et al.* 2003)

Other disruptions in APP, such as deletion or overexpression, also lead to signs of axonal transport defects. Mice that are trisomic for the chromosome encoding for APP, and thus overexpress APP, also exhibit defective retrograde

transport of NGF. (Salehi *et al.* 2006) Flies overexpressing *Drosophila* APP homolog APPL have axonal transport defects. (Torroja *et al.* 1999; Gunawardena and Goldstein 2001) Mice that have mutations leading to loss of APP function exhibit decreased axonal transport, plus kinesin subunits are decreased in axons and increased cell bodies. (Kamal *et al.* 2001) Flies with loss of APPL exhibit axonal accumulations. (Gunawardena and Goldstein 2001) Thus, disruptions to APP, such as mutation, overexpression, or deletion, can affect axonal transport.

APP interaction with motor protein kinesin I could offer a mechanistic explanation for the axonal transport defects observed in AD and animal models with APP disruptions. Previous research in the Goldstein lab suggests that APP secretase processing components are co-transported in the same axonal vesicle as APP and that APP even interacts with kinesin I subunit KLC1, which is responsible for cargo vesicle recognition, specificity, and binding. (Kamal *et al.* 2000; Kamal *et al.* 2001) This suggests that APP acts as a receptor for kinesin I. Such a model might help explain the defects in axonal transport observed when APP is mutated, overexpressed, or lost. When APP is disrupted, it could alter its association with the motor protein to disrupt its axonal transport. It would also help to explain how reduced dosage of kinesin I exacerbates the defects observed with APP mutation and overexpression. (Gunawardena and Goldstein 2001;

Stokin *et al.* 2005) Transgenic APP mice possess axonal swellings, but axonal swellings, A $\beta$  generation, and amyloid plaque deposition increase when overexpressed FAD Swedish mutant APP is combined with an otherwise benign 50% genetic reduction in KLC1. Flies overexpressing APPL or FAD mutant human APP isoform 695 also show an increase in axonal accumulations upon combination with reduced kinesin I subunit kinesin heavy chain (KHC). Thus, disruptions in APP lead to disrupted axonal transport that is enhanced with reduced motor protein machinery, possibly by interfering with normal APP association with motor proteins.

Thesis work described in this chapter set out to ask if mutations at the  $\beta$ -secretase cleavage site of APP, where the FAD Swedish mutations to APP are located, can alter axonal transport of APP. We used live cell imaging of APP tagged with yellow fluorescent protein (APP-YFP) as an experimental system to ask this question. The Goldstein lab has previously shown that APP-YFP undergoes long-distance axonal transport in mammalian hippocampal neurons, allowing us to ask what changes occur to axonal transport properties of APP-YFP when processing mutations are inserted.



## Methods

### Constructs

Bacterial plasmid pcdna3 uses a CMV promoter to encode for APP<sup>695</sup> with yellow fluorescent protein fused to the C-terminus (APP-YFP). (Kaether *et al.* 2000) With the use of QuikChange II XL site-directed mutagenesis kit (Stratagene), mutations were targeted to the two amino acids immediately adjacent to the  $\beta$ -secretase cleavage site of APP to create 2 new constructs. The first mutant construct contained the FAD Swedish mutations (K595N and M596L), while the second mutant construct contained the MV mutation (M596V). (Figure 2.1)

### Cultures

Primary hippocampal cultures were prepared by dissecting brains from wild type, newborn C57BL/J6 mice on post-natal day 1. Dissection buffer consisted of HBSS with glucose, HEPES, and antibiotics. Isolated hippocampi were incubated in a .22 $\mu$ m-filtered mixture of 45U papain (Worthington) in PBS, DL-cystein HCl (Sigma), bovine serum albumin, and D-glucose (Sigma) enriched with .05% of DNase (Boehringer Mannheim) for 20 minutes at 37°C. Hippocampi were triturated by pipetting carefully in DMEM with 10% FBS. Cells were grown in 500 $\mu$ M L-glutamine and neurobasal media supplemented with B27

(Invitrogen) over poly-L-lysine-coated coverslips and stored in a 37°C incubator with 5% CO<sub>2</sub>. SH-SY5Y cultures were grown in F-12 nutrient and Hamm media supplemented with 10% FBS.

### **Transfection and drug treatment**

After 10 days in culture, hippocampal neurons were transfected for 2 hours with 800ng wild-type or mutant DNA per well of a 24-well plate. Low transfection efficiency was obtained using Lipofectamine 2000 (Invitrogen). Experiments were designed to collect data from control and experimental groups in parallel. From a single 24-well plate of cultured hippocampal neurons, half the wells were transfected with wild-type APP-YFP, while the other half was transfected with mutant APP-YFP. Transfected hippocampal cultures in some experiments were treated with either  $\beta$ -secretase inhibitor II (Calbiochem) or  $\gamma$ -secretase inhibitor Compound E (Calbiochem). For drug treatment experiments, the entire plate was transfected with Swedish APP-YFP. Prior to imaging the next day, half the wells were treated with drug dissolved in DMSO, and half the wells were treated with DMSO only. SH-SY5Y cells were used for Western blot experiments because of their high transfection efficiency. They were transfected one day after splitting, following a protocol similar to hippocampal transfection.

### **Axonal APP-YFP movie collection**

APP-YFP transfected axons were located in primary hippocampal cultures using an inverted epifluorescent microscope (TE-2000U, Nikon) and a 100x oil immersion objective (Nikon, 1.4 NA, .126 microns/pixel) connected to a CCD camera (Roper Scientific). During imaging, cultures were kept at 37°C using a heated stage and 5% CO<sub>2</sub> chamber. Twelve to sixteen hours after transfection, movies of axons expressing APP-YFP were collected using Metamorph 7.0 software (Universal Imaging Corporation) run on a PC computer. Directionality was determined by tracking axons far away from cell bodies or axon termini, and individual transfected axons could be distinguished due to the low number of transfected neurons in the primary culture. Data was not collected if directionality could not be determined, or if other transfected axons intersected and obscured the view. Particles moving from cell bodies to axon termini were considered anterograde, and those moving from termini to cell bodies were considered retrograde. Continuous, 15-second movies of 150 frames with 100 millisecond exposure each frame were collected for APP-YFP axonal movement. Phase and fluorescent images of cell bodies were also collected to ensure that there were no signs of gross toxicity to the cells or substantial differences in the amount of transfected fluorescent protein present. All movies were collected

within an hour of the culture being placed in the heat- and CO<sub>2</sub>-controlled microscope incubator chamber.

### **APP-YFP movement analysis**

Using Metamorph software, a kymograph was generated for each movie to plot time on the y axis and distance on the x axis for the movement of each APP-YFP particle. Manual analyses were conducted on APP-YFP particle movement trajectories plotted on these kymographs. Percentages of anterograde, retrograde, and stationary particles were extracted by following particle movement from initial starting point to ultimate ending point along the kymographs. Segmental speeds and distances were calculated by following particle movement from starting point to ending point of a segment of movement along the kymograph that was uninterrupted by pauses or reversals in movement direction. Data analysis consisted of data collected from transfection experiments done in parallel.

### **Western blot analysis**

Protein analysis of transfected cultures was accomplished using Western blots and quantified using the Odyssey system. For each experiment, one 10cm plate of SH-SY5Y cells was transfected with each construct. The next day, cells were rinsed of culture media and scraped from the plate using phosphate

buffered saline (PBS) with a protease inhibitor cocktail (Roche). Cells were collected on ice, then pelleted by centrifuging at 4°C for 10 minutes at 2000rpm. After removing PBS, the cell pellets were resuspended and homogenized using NP-40 lysis buffer. After protein concentration was determined using the Bradford assay, an equal volume of 2x LDS sample buffer (Invitrogen) was added with  $\beta$ -mercaptoethanol to a final concentration of 4%. Equal amounts of protein samples were loaded onto 4-12% Bis-Tris gels, using SeePlus 2 as a molecular weight marker (Invitrogen), and gels ran at 90V until dye reached the end of the gel. Transfer onto nitrocellulose membranes was done at .3A for 90 minutes using 25 mM Tris-base, 190 mM Glycine, and 20% methanol. Ponceau S stain (Sigma) indicated the quality of the transfer and was used as a guide when cutting membranes into separate sections for incubation with different antibodies. Membrane blocking was performed for 1 hour at room temperature with Odyssey block in the absence of tween detergent to decrease background, while primary antibody incubation was done overnight at 4°C in Odyssey block with .25% Tween. Human-specific APP antibody 6E10 was used at 1:1000. Tubulin was used at 1:10,000 as a loading control. Secondary antibodies coupled to 800nm (green channel) and 700nm (red channel) fluorophores were diluted in Tris-buffered saline with Tween (TBST) at 1:10,000, and incubation was done for

2 hours at room temperature. Antibodies were used sequentially to detect levels of CTF-YFP and tubulin in the same membrane. Licor Odyssey scanner and software were used to collect images and measure fluorescence intensity for quantification. Intensity changes of 6E10 signal normalized to tubulin signal were calculated using Excel, and average changes across multiple experiments were plotted as normalized ratios to wild-type.

### **Statistics**

For analyses of APP-YFP movement parameters, student's t tests were used to determine significant differences between mutant and wild-type, or drug-treated and vehicle-treated. Mean percentages of movement, segmental velocities, and segmental run lengths were calculated for each movie collected. These movie means were used for statistical comparisons between groups. Graphs plot the mean for each construct or drug-treatment group, and error bars represent the standard error of the mean (SEM). Single stars indicate statistical significance with a p value less than .05, and double stars indicate a p value less than .01.

## Results

### **Mutant APP-YFP has altered $\beta$ -secretase cleavage and undergoes axonal transport**

The FAD Swedish mutations to APP are known to increase its cleavage by  $\beta$ -secretases. The MV mutation, on the other hand, inhibits its cleavage by  $\beta$ -secretases. We wanted to make sure that these mutations to the fusion protein APP-YFP affect  $\beta$ -secretase cleavage in the expected way. Western blots of cells transfected with the various constructs indicate that the amount of APP-YFP  $\beta$ -cleavage product C99-YFP changed with mutation at the  $\beta$ -secretase cleavage site of APP-YFP. (Figure 2.2) The Swedish mutations increased C99-YFP production to 1.796 times the amount generated by wild-type APP-YFP. The MV mutation, on the other hand, decreased the amount of C99-YFP to .611 times the amount generated by wild-type APP-YFP. These changes were statistically significant ( $\alpha < .05$ ,  $n=3$ ). To rule out the possibility that these changes in C99-YFP production might be due to different overall transfection amounts with each construct, we performed an experiment in which we normalized the amount of C99-YFP to the total amount of full-length APP-YFP and C99-YFP combined. A similar trend of changes in  $\beta$ -secretase cleavage was found.

APP-YFP moves in axons of transfected mouse hippocampal neurons, but axonal transport of mutant APP-YFP had not been previously demonstrated. We wanted to make sure that mutant APP-YFP still enters axons, undergoes axonal transport, and does not cause any gross abnormalities to transfected cells. Indeed, we found that axons of primary hippocampal mouse neurons transfected with either mutant APP-YFP construct demonstrated axonal transport of the fluorescently-tagged proteins. (Figure 2.3) Neither the Swedish nor the MV mutation to APP-YFP led to any gross toxicity of transfected axons or cells.

#### **The FAD Swedish mutations to APP-YFP inhibit anterograde axonal transport**

In order to test how FAD Swedish and MV mutations affect APP-YFP axonal transport properties, several hundred axons and almost 10,000 APP-YFP particles were analyzed manually.

The FAD Swedish mutations to APP increase  $\beta$ -secretase-dependent amyloidogenic cleavage of APP, which is also enhanced in sporadic AD, and lead to signs of axonal transport defects in transgenic mice. We wanted to test the hypothesis that Swedish mutant APP exhibits impaired axonal transport. We examined axonal transport properties of wild-type and Swedish mutant APP-YFP, including 80 axons and 2,138 particles, and found that the Swedish mutations impaired APP-YFP anterograde axonal transport. (Figure 2.4)



Movement analysis revealed a statistically significant decrease in the percentage of particles moving in the anterograde direction when compared to wild-type (WT=32.12%, SWE=23.62%,  $p=.017$ ). The percentage of retrogradely moving (WT=21.16%, SWE=23.07) and stationary particles (WT=46.72%, SWE=53.32%) increased, but those changes did not reach statistical significance ( $p=.59$  and  $.147$ , respectively). Thus, mutation at the  $\beta$ -secretase cleavage site of APP was able to affect APP axonal transport, and FAD mutations associated with axonal transport defects were able to impair APP anterograde axonal transport.

The Swedish mutations decreased the percentage of particles traveling in the anterograde direction, but to test if they affect other axonal transport properties, such as velocity or run length, we used the same data set to examine segments of movement. The Swedish mutations to APP-YFP did not significantly alter mean segmental velocity, which is the speed a particle travels in a given direction when uninterrupted by a pause or direction reversal. (Figure 2.5) This was the case for both anterograde (WT=2.31 $\mu$ m/s, SWE=2.24 $\mu$ m/s,  $p=.731$ ) and retrograde (WT=2.08 $\mu$ m/s, SWE=2.09 $\mu$ m/s,  $p=.935$ ) directions. Similarly, the Swedish mutations did not significantly alter mean segmental run length, or the distance a particle travels in a given direction when uninterrupted by a pause or direction reversal, in either the anterograde (WT=10.39 $\mu$ m, SWE=7.59 $\mu$ m,  $p=.304$ )

or retrograde (WT=7.09 $\mu$ m, SWE=5.84 $\mu$ m, p=.563) directions. Although the Swedish mutations decreased the percentage of particles undergoing anterograde axonal transport, they did not affect these other axonal transport parameters measured.

Because the Swedish mutations increase  $\beta$ -secretase cleavage of APP, this suggests that the changes observed in axonal transport of Swedish mutant APP-YFP are due to changes in  $\beta$ -secretase cleavage of APP-YFP. If this is the case, inhibiting  $\beta$ -secretase cleavage of Swedish mutant APP-YFP should attenuate or reverse the effects of mutation. To test this hypothesis, we utilized a  $\beta$ -secretase inhibitor and analyzed 90 axons and 1,974 particles to find that a  $\beta$ -secretase inhibitor was able to reverse the effect of the Swedish mutations alone. When Swedish APP-YFP was combined with 10 $\mu$ M  $\beta$ -secretase inhibitor and movement was compared to Swedish APP-YFP with vehicle alone, anterograde axonal transport improved. (Figure 2.6) The percentage of anterogradely moving particles increased, but this change did not quite reach statistical significance (SWE+DMSO=36.93%, SWE+ $\beta$ inh=44.17%, p=.060). The percentage of retrogradely moving particles significantly decreased (SWE+DMSO=21.68%, SWE+ $\beta$ inh=14.20%, p=.019). The percentage of stationary particles remained unchanged (SWE+DMSO=41.76%, SWE+ $\beta$ inh=41.63%, p=.976). This trend was

drug dose-dependent, with the magnitude and statistical significance of change increasing when using a higher concentration of inhibitor was used. With 40 $\mu$ M  $\beta$ -secretase inhibitor, the percentage of anterograde particles significantly increased (SWE+DMSO=25.51%, SWE+ $\beta$ inh=39.78%,  $p$ =.006); the percentage of retrograde particles significantly decreased (SWE+DMSO=22.69%, SWE+ $\beta$ inh=11.45%,  $p$ =.019); while the percentage of stationary particles still remained unchanged (SWE+DMSO=51.81%, SWE+ $\beta$ inh=48.78%,  $p$ =.500). Thus, the Swedish mutation phenotype was reversed with a  $\beta$ -secretase inhibitor, suggesting that the effect of the Swedish mutations was due to the increase in  $\beta$ -secretase cleavage.

Increased  $\beta$ -secretase cleavage impairs APP-YFP anterograde axonal transport, and a  $\beta$ -secretase inhibitor reverses that phenotype. The Swedish mutations increase  $\beta$ CTF-YFP, the C-terminal  $\beta$ -secretase cleavage product of APP-YFP, but they also increase A $\beta$  peptides, the product that forms after subsequent  $\gamma$ -secretase cleavage. To test if impaired anterograde axonal transport of Swedish APP-YFP is likely due to increased  $\beta$ CTF-YFP formation or increased A $\beta$  formation, we utilized a  $\gamma$ -secretase inhibitor and analyzed 118 axons and 3,490 particles. Analysis of the data revealed that a  $\gamma$ -secretase inhibitor worsened the effect of the Swedish mutations alone. (Figure 2.7) When

Swedish APP-YFP was combined with 100nM  $\gamma$ -secretase inhibitor and movement was compared to Swedish APP-YFP with vehicle alone, anterograde axonal transport was further impaired but did not quite reach statistical significance. The percentage of anterogradely moving particles decreased (SWE+DMSO=49.93%, SWE+ $\gamma$ inh=43.63%,  $p=.068$ ), while the percentage of retrogradely moving particles increased (SWE+DMSO=12.79%, SWE+ $\gamma$ inh=16.20%,  $p=.094$ ). The percentage of stationary particles remained relatively unchanged (SWE+DMSO=37.28%, SWE+ $\gamma$ inh=40.17%,  $p=.425$ ). This trend was drug dose-dependent, with the magnitude and statistical significance increasing with a higher concentration of inhibitor. With 5 $\mu$ M  $\gamma$ -secretase inhibitor, the percentage of anterograde particles significantly decreased (SWE+DMSO=47.67%, SWE+ $\gamma$ inh=34.74%,  $p=.002$ ); the percentage of retrograde particles significantly increased (SWE+DMSO=12.36%, SWE+ $\gamma$ inh=27.78%,  $p=.002$ ); and the percentage of stationary particles remained unchanged (SWE+DMSO=39.97%, SWE+ $\gamma$ inh=37.48%,  $p=.595$ ). Thus, the Swedish mutation phenotype was exacerbated with a  $\gamma$ -secretase inhibitor, suggesting that effect of Swedish mutations was due to increased  $\beta$ -secretase cleavage product  $\beta$ CTF-YFP, rather than increased  $\beta$ - and  $\gamma$ -secretase cleavage product  $A\beta$ .

### **The MV mutation to APP-YFP promotes anterograde axonal transport**

Results from experiments conducted with Swedish mutant APP-YFP with and without  $\beta$ - and  $\gamma$ -secretase inhibitors suggest that increasing  $\beta$ -secretase cleavage of APP-YFP impairs its axonal transport. To test further the ability of APP  $\beta$ -secretase cleavage to regulate axonal transport of APP, we examined axonal transport of MV mutant APP-YFP, which has reduced  $\beta$ -secretase cleavage. Data collected from 96 axons and 2,749 particles indicated that the MV mutation to APP-YFP promoted its anterograde axonal transport. (Figure 2.8) Movement analysis revealed a statistically significant increase in the percentage of particles moving in the anterograde direction (WT=36.26%, MV=43.62%,  $p=.007$ ). Additionally, there was a statistically significant decrease in the percentage of retrogradely moving particles (WT=25.02%, MV=20.73%,  $p=.046$ ). Stationary particles remained unchanged (WT=38.72%, MV=35.65%,  $p=.324$ ). Thus, mutations with opposing effects on  $\beta$ -secretase cleavage of APP have opposing effects on APP axonal transport. The Swedish mutations increasing  $\beta$ -secretase cleavage impaired anterograde axonal transport of APP-YFP, while the MV mutation decreasing  $\beta$ -secretase cleavage promoted anterograde axonal transport.

The MV mutation was also able to affect other axonal transport properties besides the percentage of particles traveling in each direction. It also significantly increased the mean anterograde segmental velocity (WT=2.38 $\mu$ m/s, MV=2.98 $\mu$ m/s,  $p=0.026$ ), but not the mean retrograde segmental velocity (WT=2.45 $\mu$ m/s, MV=2.52 $\mu$ m/s,  $p=0.905$ ). (Figure 2.9) Likewise, mean segmental run length was significantly increased in the anterograde direction only (WT=7.31 $\mu$ m, MV=14.68 $\mu$ m,  $p=0.004$ ), but mean retrograde run length remained unchanged (WT=5.19 $\mu$ m, MV=5.95 $\mu$ m,  $p=0.476$ ). Data support the hypothesis that mutation at the  $\beta$ -secretase cleavage site of APP can regulate its axonal transport.

If the effects of the MV mutation on APP-YFP axonal transport are due to its reduced  $\beta$ -secretase cleavage, and if the effects of a  $\beta$ -secretase inhibitor on Swedish mutant APP-YFP are specific to  $\beta$ -secretase inhibition, we do not expect a  $\beta$ -secretase inhibitor to alter significantly the axonal transport phenotype of the MV mutation. MV mutant APP-YFP already has inhibited  $\beta$ -secretase cleavage, so a  $\beta$ -secretase inhibitor is not expected to alter significantly its  $\beta$ -secretase cleavage or change its axonal transport properties. Analysis of 62 axons and 682 particles reveals that this is, in fact, the case. When MV mutant APP-YFP was combined with 40 $\mu$ M  $\beta$ -secretase inhibitor and movement was compared to MV mutant APP-YFP with vehicle alone, no statistically significant changes were

observed. (Figure 2.10) The percentage of anterogradely moving (MV+DMSO=42.76%, MV+ $\beta$ inh=45.31%,  $p=.510$ ), retrogradely moving (MV+DMSO=21.66%, MV+ $\beta$ inh=18.49%,  $p=.290$ ), and stationary particles remained relatively unchanged (MV+DMSO=35.59%, MV+ $\beta$ inh=36.20%,  $p=.877$ ). Thus, the MV mutation to APP-YFP not only increased the percentage of anterograde and decreased the percentage of retrograde particles, but it also increased segmental velocity and segmental run length in the anterograde direction specifically.

### **Mutations to APP-YFP do not alter its axonal entry**

Because the Swedish and MV mutations change  $\beta$ -secretase cleavage and axonal transport of APP-YFP, we wanted to test if they alter axonal entry of APP-YFP. One effect of increased  $\beta$ -secretase cleavage could be that fewer APP-YFP vesicles that enter the axon, while decreased  $\beta$ -secretase cleavage could increase the number of APP-YFP vesicles in the axon. Analyses of the same data sets collected for transport experiments indicated that the mean number of mutant APP-YFP vesicles per length of axon did not change compared to WT for either the Swedish (WT=.287 particles/ $\mu$ m, SWE=.322 particles/ $\mu$ m,  $p=.166$ ) or the MV (WT=.276 particles/ $\mu$ m, MV=.299 particles/ $\mu$ m,  $p=.368$ ) mutation. (Figure 2.11) Another possibility is that the number of APP-YFP proteins loaded into each

transport vesicle could change with mutation. One approach to test this is to measure the mean fluorescence intensities of wild-type and mutant APP-YFP particles. Data reveal that there is no significant difference in mutant APP-YFP particle fluorescence intensity when normalized to WT (Swedish=.896,  $p=.572$  and MV=.876,  $p=.381$ ). Thus, it does not appear that mutations to APP-YFP alter its axonal entry by these measures.



## Discussion

We aimed to examine the effects of mutations to APP on its axonal transport properties, using a neuronal system and examining hundreds of axons and thousands of particles. We tested the hypotheses that 1)  $\beta$ -secretase cleavage can regulate APP axonal transport and 2) FAD mutations can impair axonal transport of APP.

Mutations at the  $\beta$ -secretase cleavage site of APP can alter its axonal transport properties. The FAD Swedish mutations, which increase  $\beta$ -secretase cleavage of APP, inhibited anterograde axonal transport of APP-YFP by decreasing the percentage of particles moving in the anterograde direction to a -26.48% change from wild-type. (Figure 2.12) The MV mutation, which decreases  $\beta$ -secretase cleavage of APP, exerted an opposing effect by promoting APP-YFP anterograde axonal transport. The MV mutation increased the percentage of particles traveling in the anterograde direction to a 20.30% change from wild-type and decreased the percentage of particles traveling in the retrograde direction to a -17.15% change from wild-type. The MV mutation also increased mean anterograde segmental velocity 25.21% and mean anterograde segmental run length 100.90% compared to wild-type. (Figure 2.13)

These opposing effects on axonal transport properties seen with opposing mutations at the  $\beta$ -secretase cleavage site of APP suggest that phenotypic differences observed are, in fact, due to changes in  $\beta$ -secretase cleavage of APP. This interpretation is further supported by the ability of a  $\beta$ -secretase inhibitor to reverse the Swedish mutation phenotype by increasing the percentage of anterograde transport to a 55.95% change from control (Figure 2.12), whereas the Swedish mutations alone had decreased it.

The Swedish mutations that disrupt APP axonal transport lead to increased  $\beta$ CTFs that result from  $\beta$ -secretase cleavage of APP, but these mutations also lead to increased  $A\beta$  peptides that result after subsequent  $\gamma$ -secretase cleavage. Previous research has argued that  $A\beta$  peptides induce defects in axonal transport. Several cell culture studies have shown defects in anterograde and retrograde axonal transport of mitochondria and dense core vesicles with incubation of  $A\beta$ . These defects involve GSK3 $\beta$  and NMDA signaling, cytoskeletal disruption, or actin aggregation. (Rui *et al.* 2006; Vossel *et al.* 2010; Decker *et al.* 2010; Pigino *et al.* 2009; Pigino *et al.* 2003; Hiruma *et al.* 2003) Additionally, FAD PS1 mice with an increased ratio of  $A\beta_{42}/A\beta_{40}$  show decreased densities of synaptic protein-containing vesicles within neurites in

culture and decreased APP amounts in peripheral nerves. Thus, it appears that A $\beta$  is able to impair axonal transport.

Defects in axonal transport can also occur independently of A $\beta$ . Previous research has shown that the axonal swellings that develop in TgAPP<sup>Swe</sup> mice do so independently of A $\beta$ . TgAPP<sup>Swe</sup> mice did not exhibit enhanced axonal swellings either when combined with transgenic FAD PS1 expression to increase A $\beta$ <sub>42</sub>/A $\beta$ <sub>40</sub> ratios, or when combined with transgenic expression of A $\beta$  peptides fused to dementia-related BRI proteins to elevate overall A $\beta$  amounts. (Stokin *et al.* 2008)

Several pieces of evidence support that the defects in Swedish mutant APP-YFP axonal transport observed in this study occur independently of A $\beta$ . First, when Swedish APP-YFP was combined with a  $\gamma$ -secretase inhibitor, which decreases A $\beta$  generation compared to the Swedish mutations alone, the impaired axonal transport phenotype was exacerbated, rather than alleviated. The percentage of anterogradely moving particles decreases to a -27.12% change from control, and the percentage of retrogradely moving particles increases to a 124.77% change from control. (Figure 2.12) This suggests that the defects in APP axonal transport observed do not result from A $\beta$  peptides, since decreasing A $\beta$  with a  $\gamma$ -secretase inhibitor did not alleviate the impaired axonal transport

phenotype. However, using a  $\gamma$ -secretase inhibitor also has the secondary effect of increasing  $\beta$ CTFs, which prevents straightforward interpretation of these data. Second, the Swedish mutations specifically affected anterograde axonal transport, unlike previously reported  $A\beta$ -induced axonal transport defects that affect anterograde and retrograde transport. Also, the Swedish mutations did not change the number of particles that were undergoing axonal transport or the velocity of those particles, as other research has indicated  $A\beta$  does. The studies conducted on  $A\beta$ -induced defects on axonal transport use at least nM concentrations of  $A\beta$ , while preliminary MesoScale Discovery measurements on Swedish APP-YFP culture media from experiments described in this chapter indicated below pM concentrations of  $A\beta_{42}$  and pM concentrations of  $A\beta_{40}$ . Thus, it appears that FAD Swedish mutations may impair APP anterograde axonal transport by an  $A\beta$ -independent mechanism. Research conducted by other groups has previously identified AD-related pathology that is  $\beta$ CTF-dependent and  $A\beta$ -independent. (Jiang *et al.* 2010)

Defects in APP axonal transport could result from increased  $\beta$ -secretase cleavage not only by FAD mutation, but also through other alterations in APP demand or function. FAD mutations only account for a very small percentage of AD cases, but aberrant APP processing is a common feature to the disease and

can arise independent of genetic mutation.  $\beta$ -secretase cleavage of APP could become dysregulated and lead to defects in APP axonal transport upon changes in synaptic demands. APP processing has been shown to be important for synaptic signaling and plasticity, both of which have been shown to be impaired in animal models of amyloid pathology. (Moya *et al.* 1994; Chapman *et al.* 1999; Cirrito *et al.* 2005; Wang *et al.* 2005; Calabrese *et al.* 2007; Tampellini *et al.* 2009; Abramov *et al.* 2009; Wei *et al.* 2009) Increased demands of APP processing for synaptic function could potentially contribute to or exacerbate aberrant APP processing and axonal transport defects. Also, brain trauma leading to axonal injury leads to accumulation in axonal swellings of APP and cleavage fragments, including  $\beta$ CTFs and  $A\beta$ , suggesting that stresses to the brain that compromise axonal health could alter APP cleavage. (Kawarabayashi *et al.* 1993; Smith *et al.* 2003)

Differences in APP transport could be observed whether APP cleavage occurs in the cell body or after entering the axonal compartment. If APP processing occurs in the cell body, full-length and cleavage fragments of APP could sort into different vesicles, and each vesicle type could exhibit different transport properties. There is previous evidence to support this. (Muresan *et al.* 2009) APP transport could also be disrupted if APP proteolytic processing occurs

in the axonal compartment, and full-length and cleavage fragments of APP have different transport properties. There is evidence for axonally transported APP undergoing proteolytic processing into A $\beta$  or intermediates. (Nikolaev *et al.* 2009; Morin *et al.* 1993; Moya *et al.* 1994; Amaratunga and Fine 1995; Amaratunga *et al.* 1995; Amaratunga *et al.* 1993; Buxbaum *et al.* 1998; Tokuda *et al.* 1996; Kamal *et al.* 2001; Roher *et al.* 2002; Wirths *et al.* 2002)

The ability of  $\beta$ -secretase cleavage to regulate APP axonal transport suggests the possibility that full-length APP protein has different axonal transport properties than APP once it is cleaved. Because APP-YFP used in this study has YFP attached to the C-terminus of APP, fluorescent particles analyzed for this study could consist of full-length APP-YFP and CTF-YFP. Swedish APP-YFP undergoes increased  $\beta$ -secretase cleavage and has increased  $\beta$ CTF-YFP. MV APP-YFP, on the other hand, undergoes decreased  $\beta$ -secretase cleavage and has decreased  $\beta$ CTF-YFP. The inhibition of Swedish mutant APP-YFP anterograde axonal transport implies that  $\beta$ CTF-YFP has impaired axonal transport properties compared to full-length APP-YFP, since  $\beta$ CTF-YFP is increased with the Swedish mutations. This hypothesis is further supported by the  $\gamma$ -secretase inhibitor data. The Swedish mutations increase  $\beta$ CTFs, and the amount of  $\beta$ CTFs further increases when Swedish mutant APP-YFP is combined with a  $\gamma$ -secretase

inhibitor.  $\beta$ CTFs cannot be processed further into  $A\beta$  peptides by  $\gamma$ -secretase, and the impaired axonal transport phenotype of the Swedish mutations alone is exacerbated. A way to test this hypothesis more directly would be to examine axonal transport of  $\beta$ CTF itself.  $\beta$ -secretase cleavage of APP-YFP generates a  $\beta$ CTF that is 99 amino acids long and still has YFP attached (C99-YFP). Axons of neurons transfected with a C99-YFP construct would be expected to exhibit reduced anterograde axonal transport compared to axons transfected with wild-type APP-YFP, which would have a mixed population of full-length APP-YFP and CTF-YFP. Such a result would support the hypothesis that full-length APP-YFP has different axonal transport properties than  $\beta$ -cleavage product C99-YFP.

APP  $\beta$ -secretase cleavage site mutations could regulate APP axonal transport if these mutations change APP association with anterograde motor protein kinesin I. APP is a transmembrane protein, shown to be present in axonal membrane vesicles and interact with KLC1. It undergoes axonal transport, and alterations in APP can lead to signs of axonal transport defects. A model has been proposed with APP acting as a motor protein receptor on a cargo vesicle, which is consistent with its impaired axonal transport upon mutation. Increased  $\beta$ -secretase cleavage of APP could decrease the amount of APP associated with kinesin and undergoing anterograde axonal transport, if  $\beta$ CTFs have decreased

association with kinesin compared to full-length APP. This would explain why Swedish mutant APP-YFP has decreased and MV mutant APP-YFP has increased anterograde axonal transport. Because both full-length APP-YFP and the  $\beta$ -cleavage product  $\beta$ CTF-YFP would still possess the C-terminus of APP shown to interact with KLC1, it is not obvious why full-length APP-YFP may exhibit different axonal transport properties than  $\beta$ CTF-YFP. Perhaps, the N-terminal domain of APP plays a role in how the protein interacts with KLC1. The N-terminal domain of APP is involved in forming dimers. (Gralle *et al.* 2009; Soba *et al.* 2005; Wang and Ha 2004; Scheuermann *et al.* 2001) An interesting untested possibility is that the formation of APP dimers or multimers on transport vesicles enhances APP interaction with kinesin motor proteins.

This notion of mutations to APP changing its association with kinesin motor proteins could provide an explanation for why MV mutant APP-YFP shows increased anterograde segmental velocity. Because inhibited  $\beta$ -secretase cleavage would provide a greater opportunity for APP-YFP to remain as a full-length protein, possibly there is an increased association of MV mutant APP-YFP with anterograde kinesin I motors. If multiple full-length MV mutant APP-YFP particles were to reside on the membrane of a transport vesicle, this could possibly cause an increased recruitment of kinesin motors to the vesicle and lead



to an increase in anterograde velocity. Though *in vitro* studies suggest kinesin to be a highly processive motor, recent research conducted *in vivo* suggests that kinesin might be poorly processive. (Reis 2008) If kinesin were a poorly processive motor, it would allow changes in kinesin number to affect velocity, providing one possible explanation for the MV mutation's ability to increase anterograde velocity.

In conclusion, this study has demonstrated that 1)  $\beta$ -secretase cleavage of APP can regulate APP axonal transport and 2) FAD mutations can impair APP axonal transport. These findings present  $\beta$ -secretase processing of APP as a novel mechanism for APP axonal transport regulation. It also suggests increased  $\beta$ -secretase processing and impaired axonal transport of APP as a possible mechanism underlying the axonal defects observed in AD, a hypothesis further explored in the following chapter.

This chapter is currently being prepared for submission and publication of the material. Rodrigues EM and Goldstein LSB. The dissertation author was the primary author and investigator of this paper.

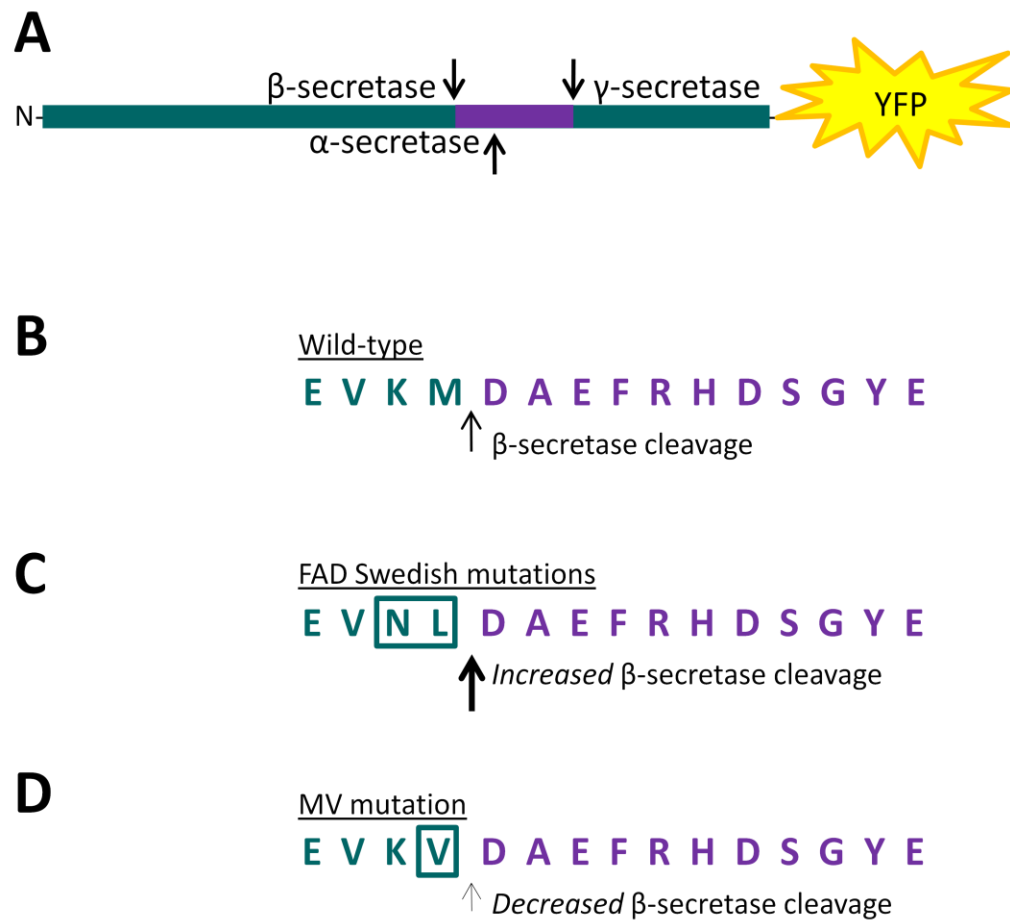


Figure 2.1. APP-YFP and mutations. A) APP<sup>695</sup> has YFP attached to the C-terminus. B) The amino acid sequence flanking the  $\beta$ -secretase cleavage site for wild-type APP-YFP is shown.  $\beta$ -secretase cleaves at the location indicated by the arrow. C) The FAD Swedish mutations at the  $\beta$ -secretase cleavage site of APP-YFP consist of K595N and M596L mutations, which increase  $\beta$ -secretase cleavage. D) The MV mutation at the  $\beta$ -secretase cleavage site of APP-YFP consists of an M596V mutation, which decreases  $\beta$ -secretase cleavage.

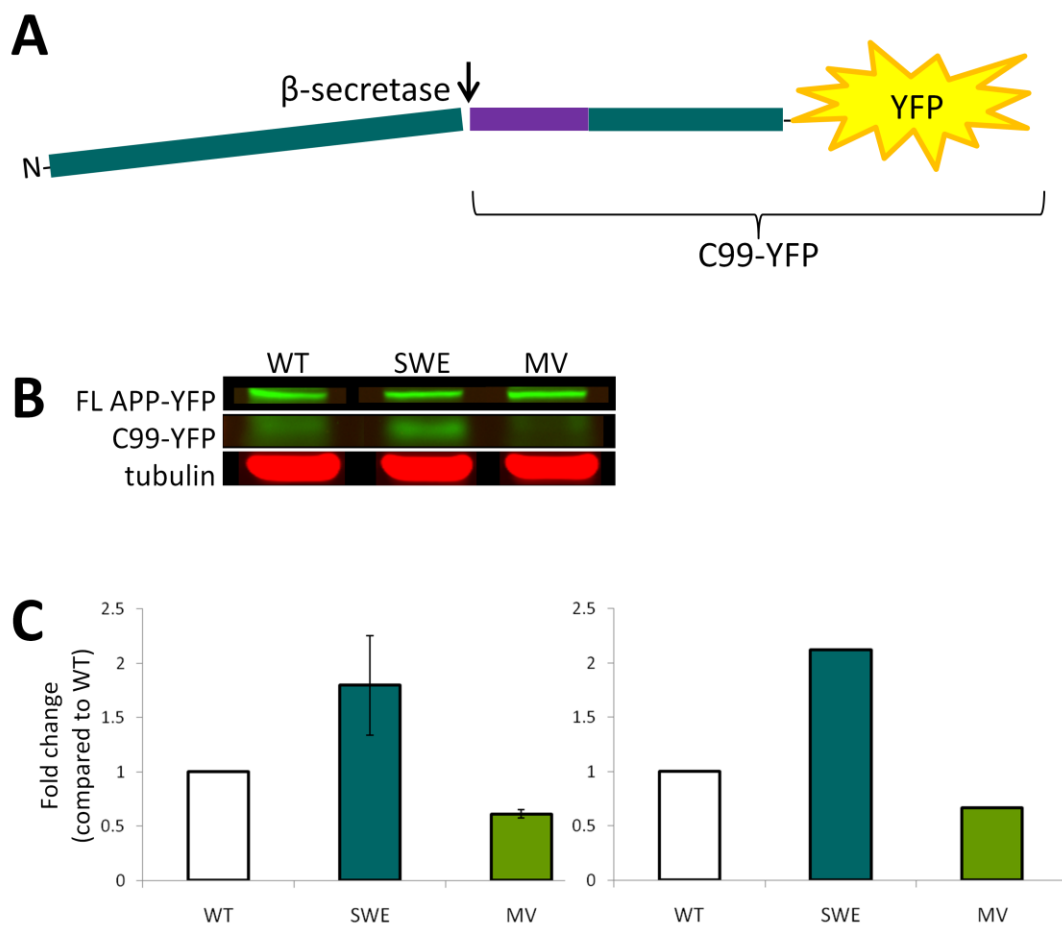


Figure 2.2. Mutations of APP-YFP that alter  $\beta$ -secretase cleavage. A)  $\beta$ -secretase cleavage of APP-YFP generates a CTF 99 amino acids long with YFP attached (C99-YFP). B) SH-SY5Y cells were transfected with wild-type, Swedish, or MV APP-YFP, and 20 $\mu$ g protein were loaded onto a Western blot. Example bands of 6E10 reactivity are shown for full-length APP-YFP (FL APP-YFP) and C99-YFP. Tubulin was used as a loading control. C) Quantification of Western blot analysis. Left graph shows quantification of C99-YFP, indicating an increase from wild-type with the Swedish mutations and a decrease with the MV mutation. (n=3) Right graph shows quantification of the ratio of C99-YFP to C99-YFP plus FL APP-YFP in one experiment. Similar effects of mutations are revealed, indicating no significant differences in transfection amount with the various constructs.

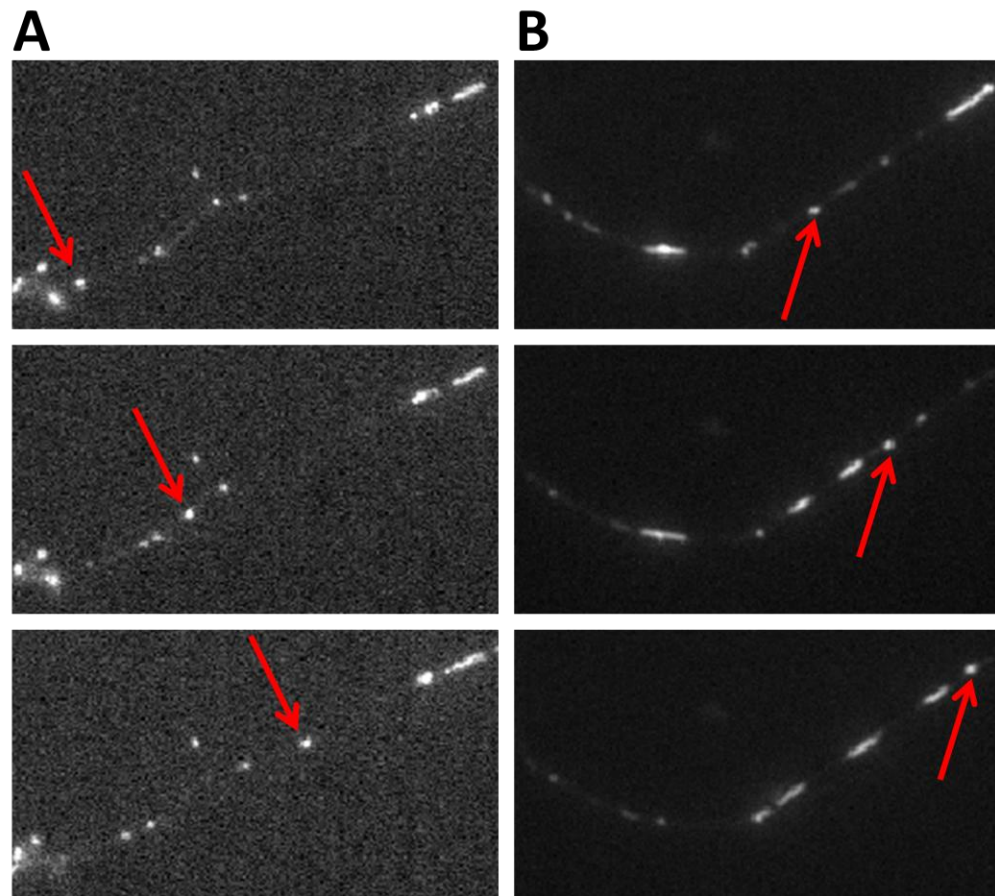


Figure 2.3. Mutant APP-YFP undergoes axonal transport. A) An axon transfected with Swedish APP-YFP is shown. The red arrows follow a single particle as it travels in the anterograde direction across chronological frames (top to bottom) of a single movie. B) MV APP-YFP similarly shows axonal transport.

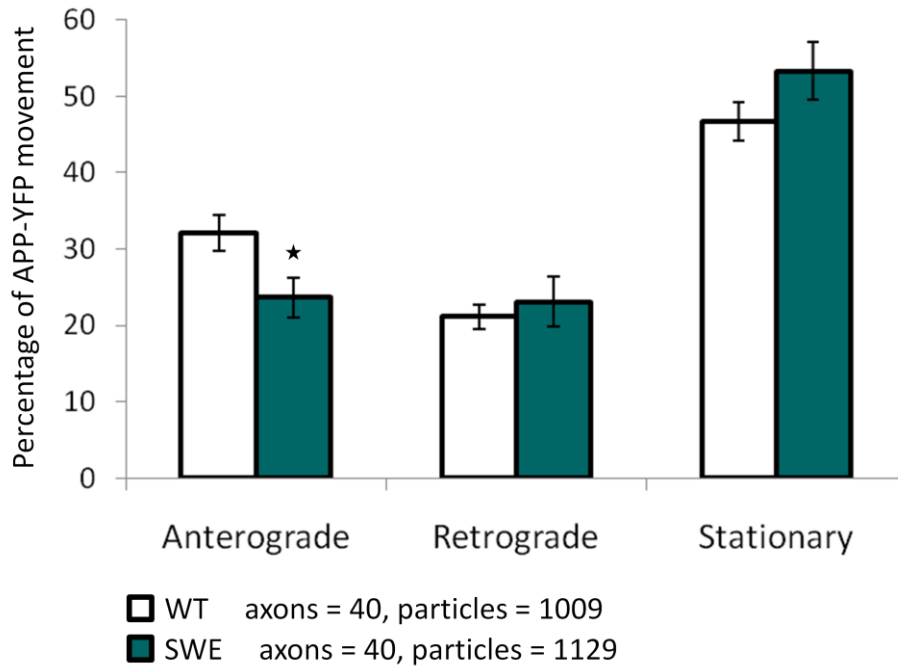


Figure 2.4. Effect of Swedish mutations on percentages of APP-YFP movement. Analysis of the percentages of APP-YFP particles moving in each direction revealed that the Swedish mutations significantly reduced the percentage of particles traveling in the anterograde direction. ( $p < .05$ )

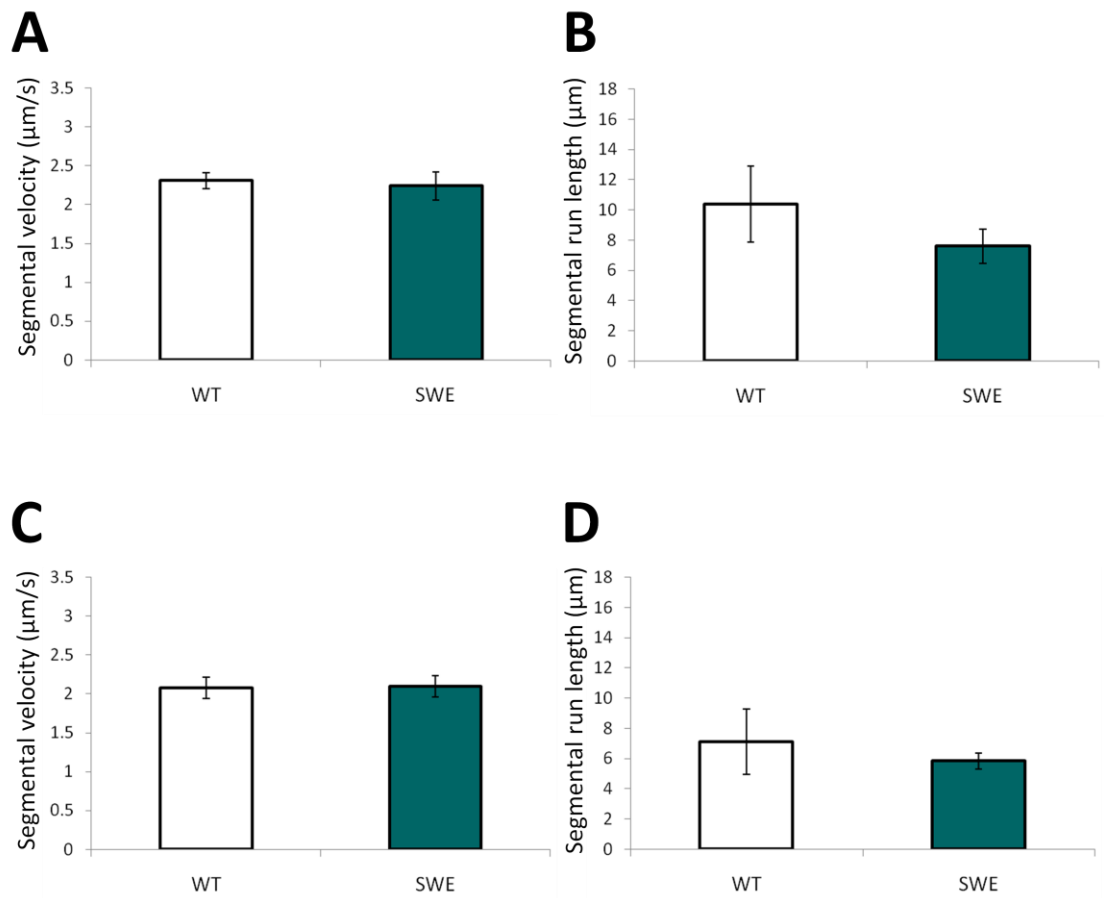


Figure 2.5. Effect of Swedish mutations on segmental velocities and segmental run lengths. Analyses of segmental velocities and segmental run lengths in the anterograde (A and B) and retrograde (C and D) directions revealed no significant effects of the Swedish mutations.

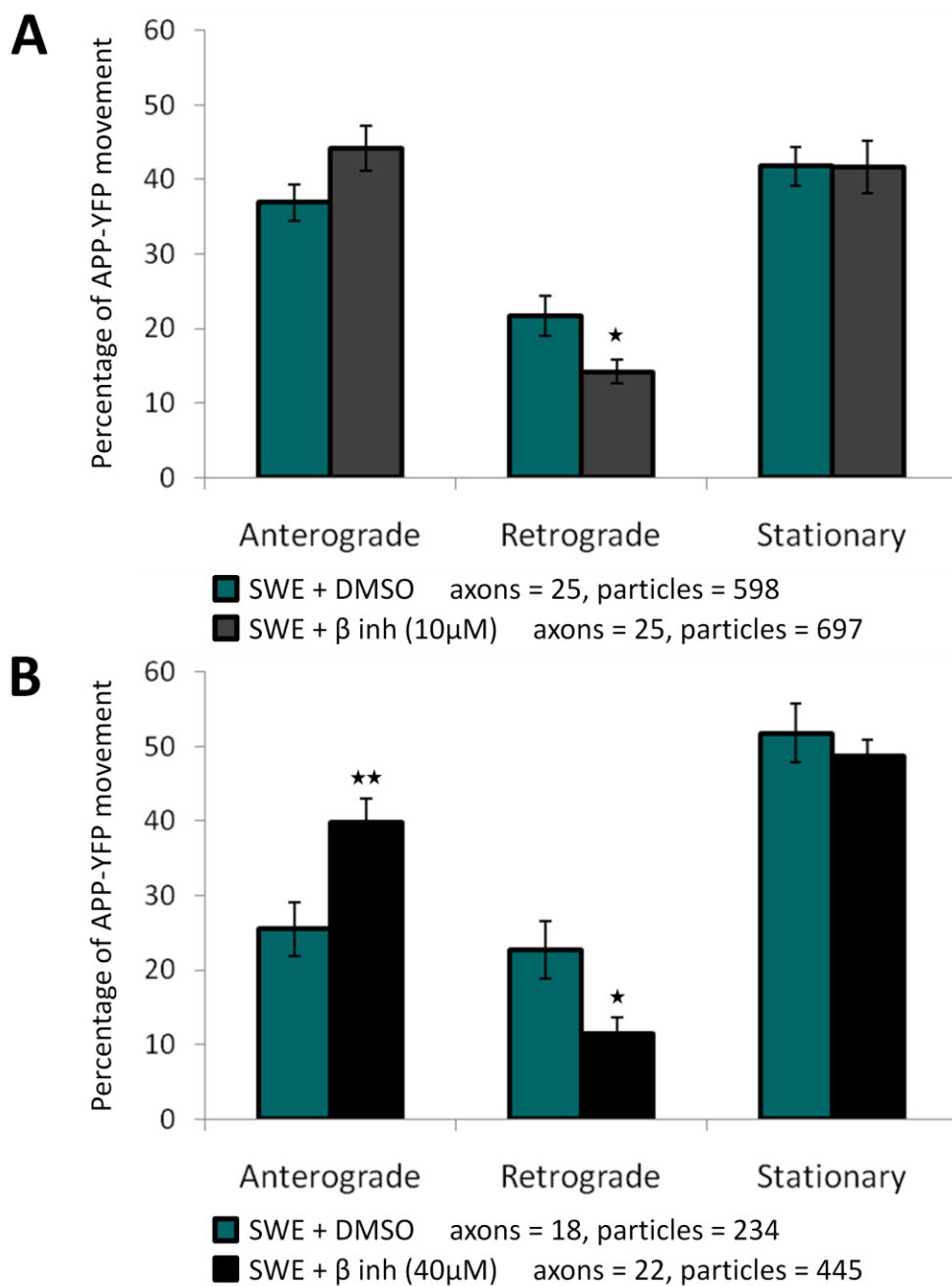


Figure 2.6. Effect of  $\beta$ -secretase inhibitor on percentages of Swedish APP-YFP movement. A) 10 $\mu$ M  $\beta$ -secretase inhibitor significantly reduced the percentage of particles moving in the retrograde direction ( $p < .05$ ). B) A higher concentration of 40 $\mu$ M  $\beta$ -secretase inhibitor further improved anterograde transport. The percentage of particles moving in the anterograde direction significantly increased ( $p < .01$ ), while the percentage of particles moving in the retrograde direction decreased ( $p < .05$ ).

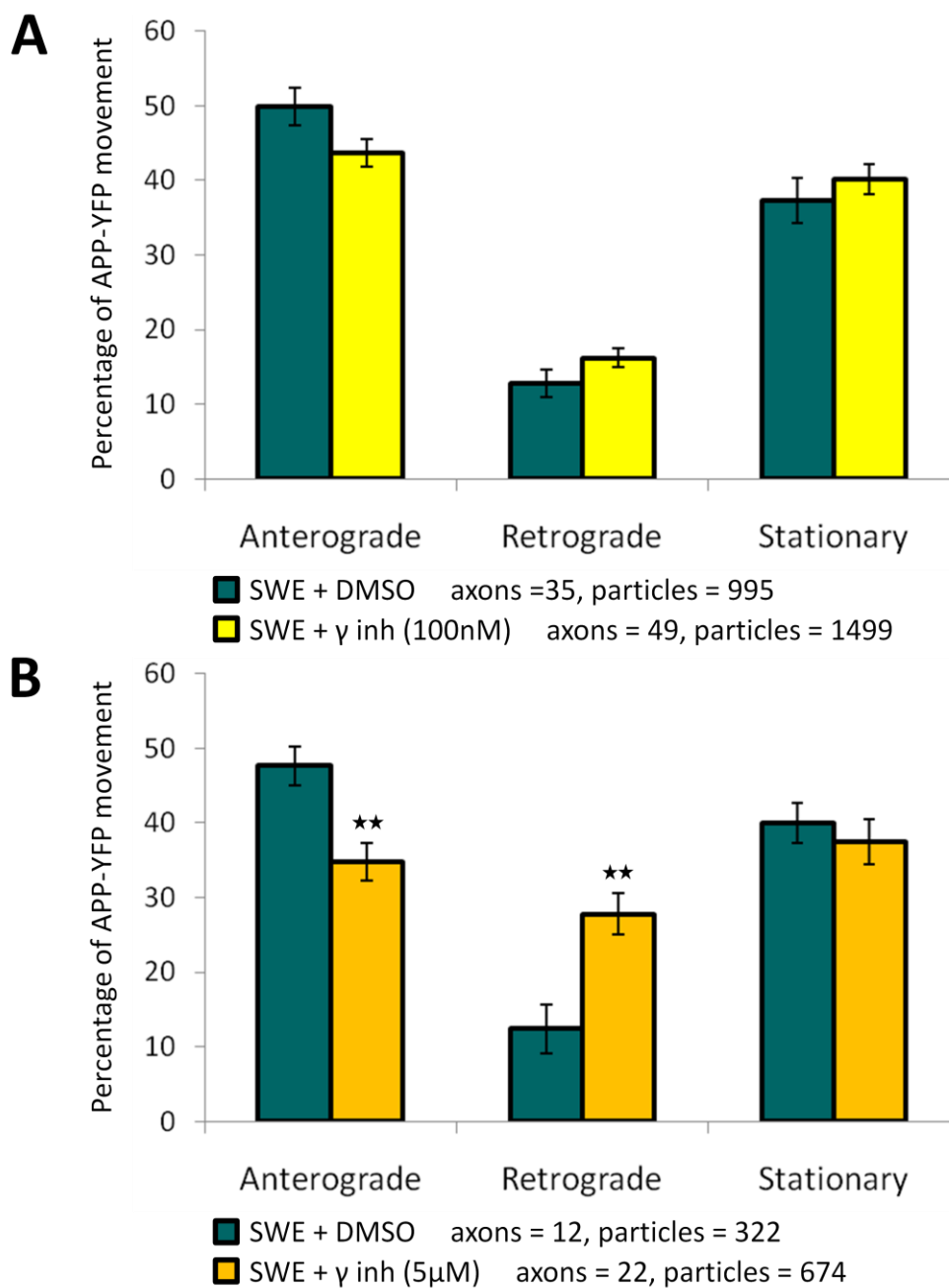


Figure 2.7. Effect of  $\gamma$ -secretase inhibitor on percentages of Swedish APP-YFP movement. A) 100nM  $\gamma$ -secretase inhibitor did not significantly alter percentages of Swedish APP-YFP movement. B) A higher concentration of 5 $\mu$ M  $\gamma$ -secretase inhibitor worsened the transport phenotype of the Swedish mutations. The percentage of particles moving in the anterograde direction significantly decreased ( $p < .01$ ), while the percentage of particles moving in the retrograde direction increased ( $p < .01$ ).



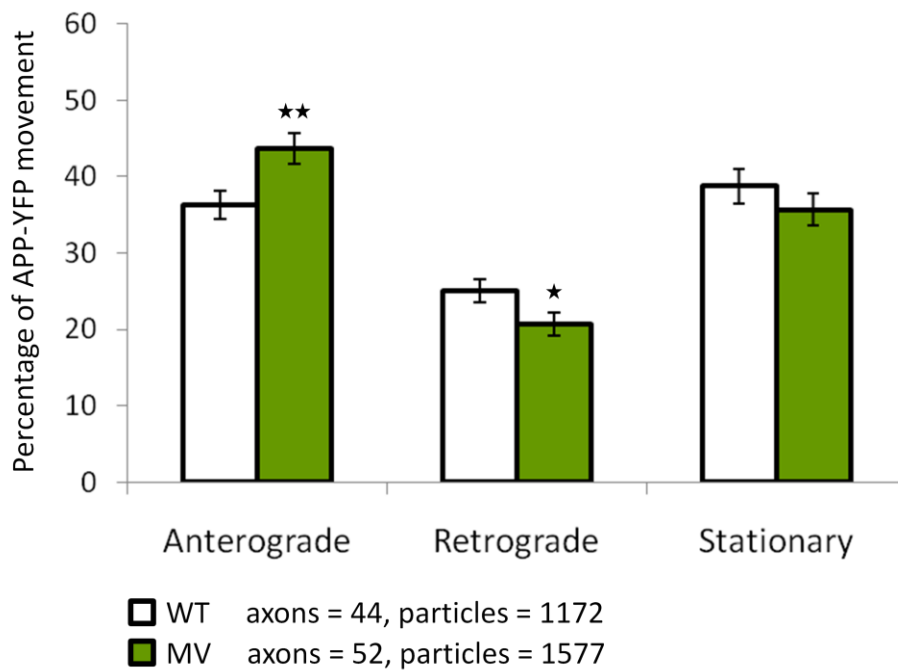


Figure 2.8. Effect of MV mutation on percentages of APP-YFP movement. Analysis of the percentages of APP-YFP particles moving in each direction revealed that the MV mutation significantly increased the percentage of particles traveling in the anterograde direction ( $p < .01$ ) and decreased the percentage of particles moving in the retrograde direction ( $p < .05$ ).

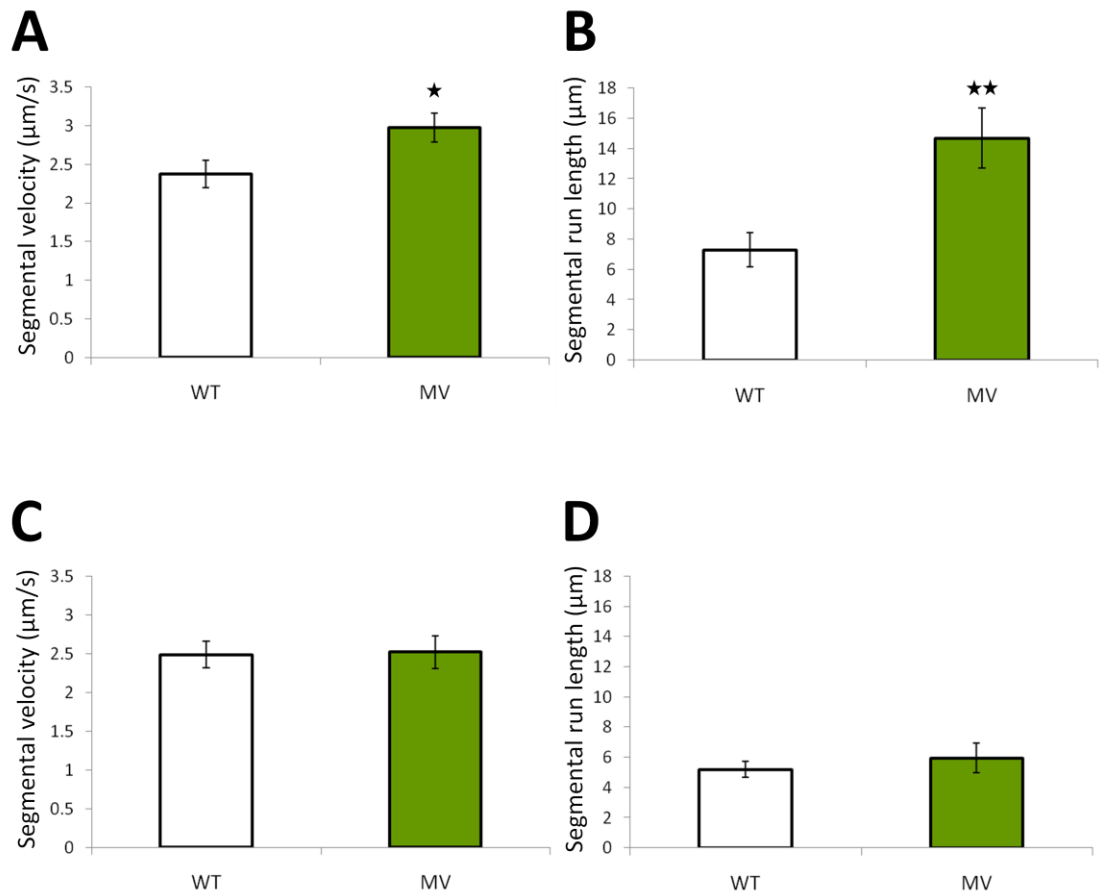


Figure 2.9. Effect of MV mutation on segmental velocities and segmental run lengths. Analyses of segmental velocities and segmental run lengths revealed a significant increase in anterograde segmental velocity (A,  $p < .05$ ) and anterograde segmental run length (B,  $p < .01$ ) for MV APP-YFP. No significant effects of the MV mutation were found in the retrograde direction (C and D).

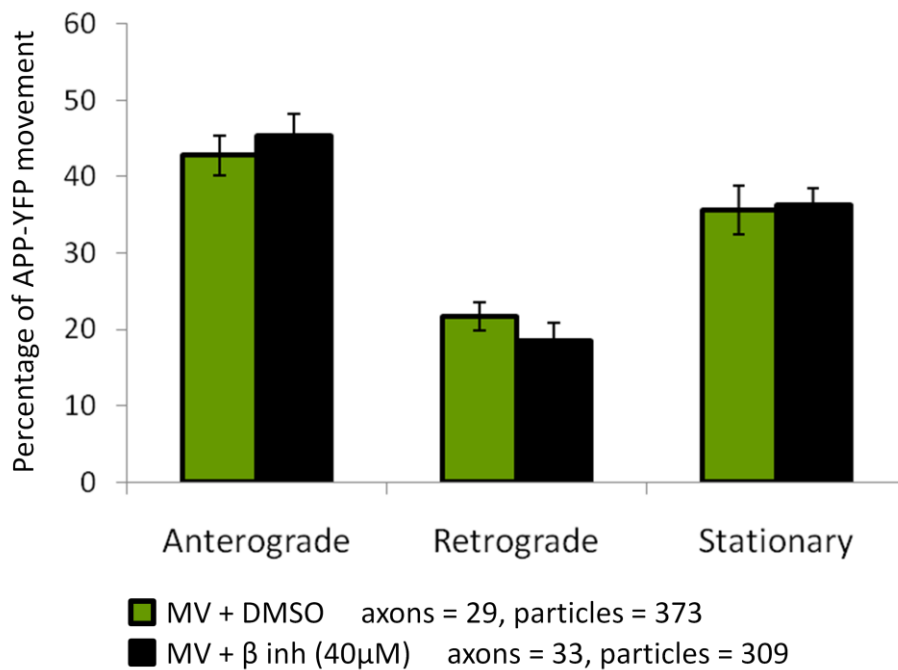


Figure 2.10. Effect of  $\beta$ -secretase inhibitor on percentages of MV APP-YFP movement. 40 $\mu$ M  $\beta$ -secretase inhibitor did not affect the percentage of MV APP-YFP particles moving in either direction or remaining stationary.

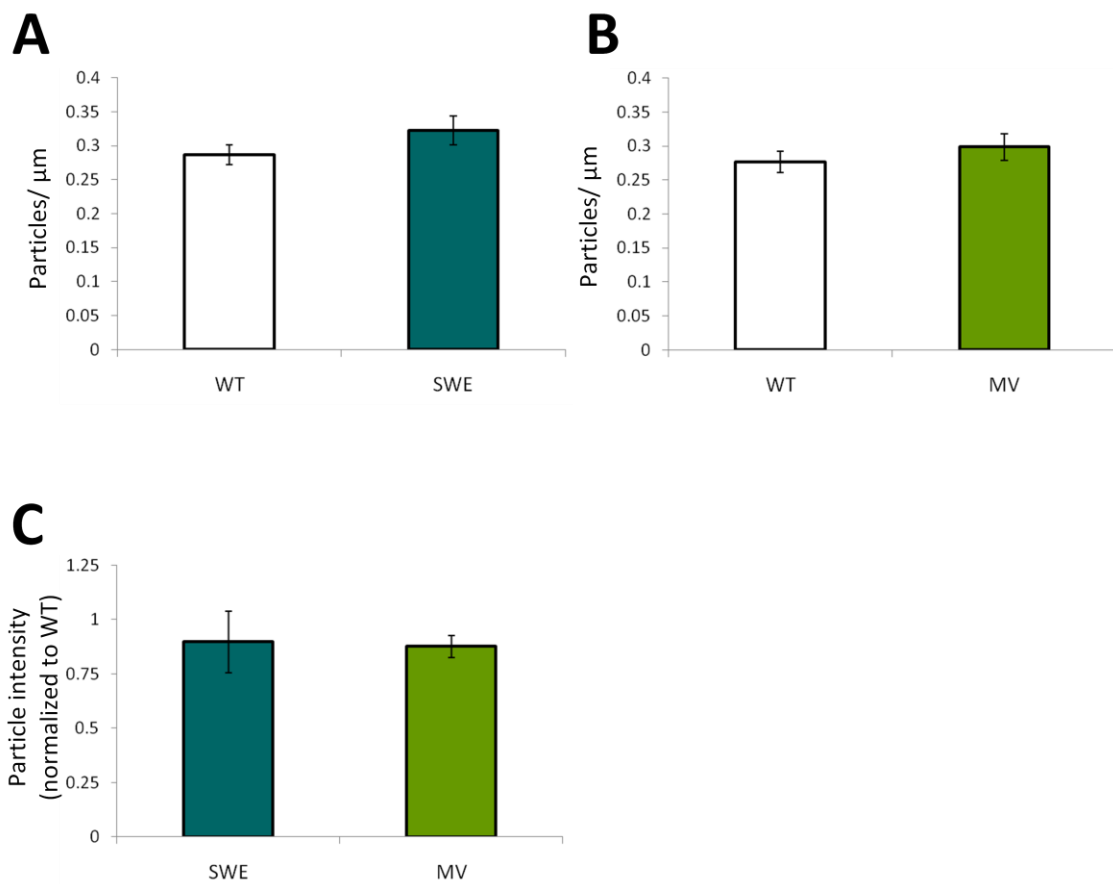


Figure 2.11. Effect of mutations on axonal APP-YFP vesicle number and fluorescence intensity. Neither the Swedish (A) nor the MV (B) mutation affected the number of APP-YFP particles in axons. C) The mean fluorescence intensity of APP-YFP vesicles did not change with either the Swedish or MV mutations.

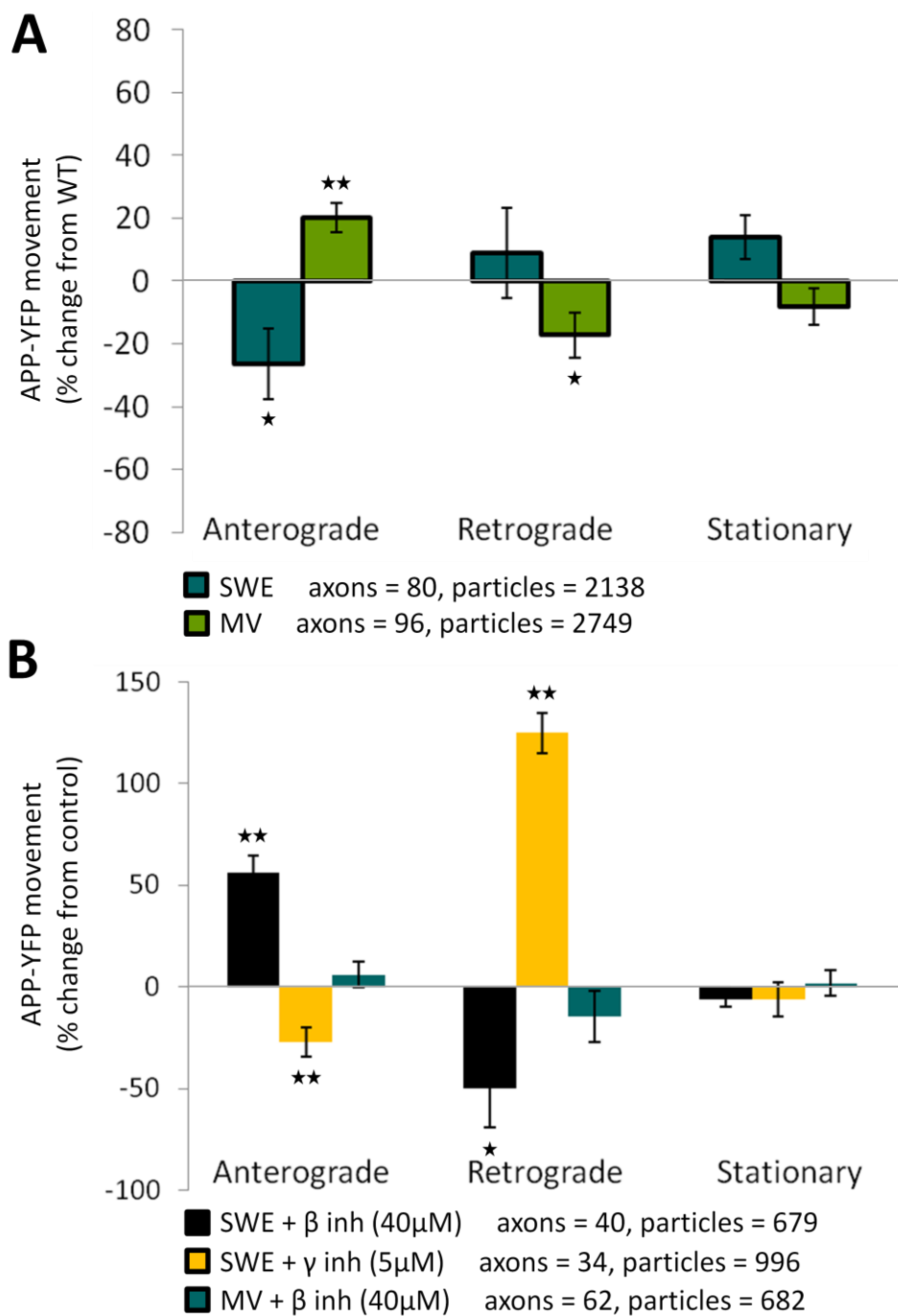


Figure 2.12. Opposite effects of Swedish and MV mutations on percentages of movement. A) The Swedish mutations decreased APP-YFP anterograde transport, while the MV mutation increased it. B)  $\beta$ -secretase inhibitor improved anterograde transport of Swedish APP-YFP, while  $\gamma$ -secretase inhibitor worsened anterograde transport of Swedish APP-YFP.  $\beta$ -secretase inhibitor did not affect MV APP-YFP transport. N's are for DMSO and drug-treated groups combined.

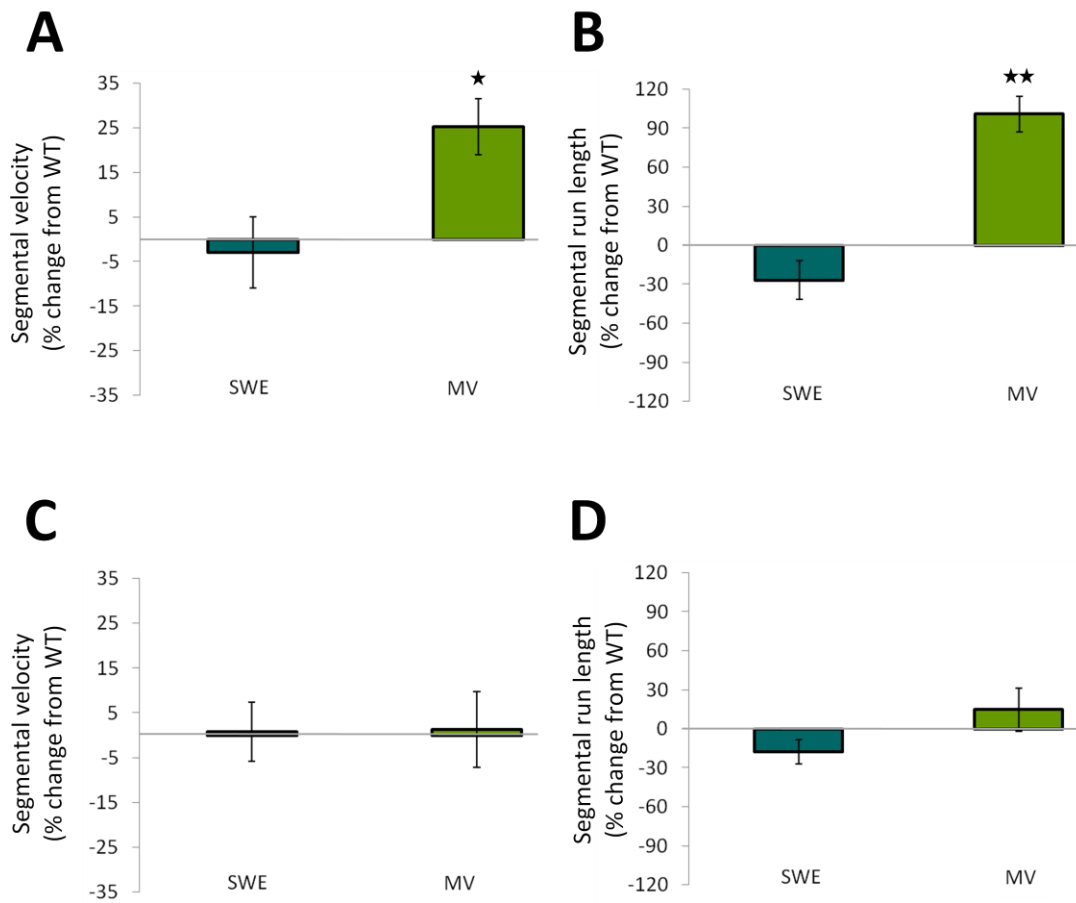


Figure 2.13. MV mutation specifically affects anterograde segmental velocity and segmental run length. The Swedish mutations had no effect, but the MV mutation significantly increased both anterograde segmental velocity (A) and anterograde segmental run length (B). Neither the Swedish nor the MV mutation affected retrograde segmental velocity (C) or run length (D).

Chapter III -

AXONAL DEFECTS IN AN FAD SWEDISH MUTANT APP GENE-TARGETED  
MOUSE

**Abstract**

The FAD Swedish mutations to APP, which enhance its cleavage by  $\beta$ -secretase, have been shown to disrupt axonal transport of APP *in vitro*, as described in Chapter II. The same mutations to APP have previously been described to cause axonal swellings, an indicator of disrupted axonal transport, in TgAPP<sup>Swe</sup> mice that overexpress FAD Swedish mutant APP. These axonal swellings also develop in human sporadic AD brains well before amyloid plaques deposit. Research described in this chapter demonstrates that the FAD Swedish mutations in the mouse APP gene, along with a humanized A $\beta$  region, are sufficient to induce axonal dystrophy *in vivo*, even when APP is expressed at endogenous levels. This axonal dystrophy, in the form of axonal dilation, also occurs before amyloid plaques deposit and does not correlate with changes in a corresponding terminal field. Thus, the FAD Swedish mutations to APP can not only cause disrupted axonal transport of APP *in vitro*, but can also lead to early axonal pathology *in vivo*. These findings support the possible contribution of defective APP axonal transport to axonal pathology observed in AD.



## Introduction

Aberrant APP processing, impaired axonal transport, and axonal dystrophy contribute to AD pathology. Aberrant APP processing in sporadic AD and in TgAPP<sup>Swe</sup> mice lead to axonal transport defects and axonal dystrophy. The FAD Swedish mutations to APP-YFP cause aberrant APP processing and impaired APP axonal transport, as demonstrated in Chapter II. Dystrophic neurites are prevalent in AD, particularly surrounding the amyloid plaques that characterize AD. Axonal swellings, which indicate disrupted axonal transport, are a type of axonal dystrophy that develops well before plaques do. This poses an interesting possibility that defective axonal transport of APP could be an underlying mechanism to the early axonal transport defects and widespread axonal dystrophy that characterize AD.

Though TgAPP<sup>Swe</sup> mice develop axonal swellings, it remains unclear if FAD mutations are sufficient, or if overexpression of the mutant protein is necessary, to induce this axonal dystrophy. Transgenic mice express the mutant APP transgene in addition to the endogenous mouse APP gene. Thus, APP is overexpressed, yet this is the type of mouse model most often used to model amyloid pathology. As previously discussed in Chapter I, overexpression, deletion, or mutation of APP can affect the axonal compartment. Research

described in this chapter asks if axonal dystrophy develops in an animal model that does not rely upon mutant APP overexpression, in order to ask more directly how the FAD Swedish mutations to APP affect the disease process *in vivo*.

A gene-targeted mouse with the FAD Swedish mutations targeted to the mouse APP gene was used in this study to investigate of the effects of mutations without possible confounding effects of protein overexpression. In addition to possessing the FAD Swedish mutations, this gene-targeted mouse model also possesses mutations in the mouse APP gene in the region encoding for A $\beta$ .

(Figure 3.1) These mutations serve to make the A $\beta$  region of the mouse APP protein homologous to that of the A $\beta$  region of the human APP protein. This is an important change to make, since mouse A $\beta$  does not aggregate into amyloid plaques. Humanizing the mouse A $\beta$  region permits study of the effects of increased amyloidogenic processing of APP and presence of human A $\beta$ , without possible confounding effects of having the mouse A $\beta$  peptide present.

Comparing phenotypes between transgenic and gene-targeted mice can help distinguish effects that are due to mutation from effects that are possibly consequences of protein overexpression.

Previous research conducted on this gene-targeted mouse reveals that the FAD Swedish mutations and a humanized A $\beta$  region without APP overexpression lead to increased  $\beta$ -secretase cleavage of APP, increased levels of human A $\beta$ , but no plaque deposition. (Reaume *et al.* 1996; Flood *et al.* 2002) Because axonal swellings develop before amyloid plaques deposit, defective axonal transport is likely an early event in disease pathogenesis. The fact that this gene-targeted mouse model does not develop amyloid plaques, despite increased  $\beta$ -secretase processing of APP and increased A $\beta$  levels, emphasizes its use as a model of the earliest changes that might occur in the disease process. To date, no axonal or synaptic characterization has been conducted.

Thesis research described in this chapter uses gene-targeted mice to test if the Swedish mutations to APP and a humanized A $\beta$  region are sufficient for axonal dystrophy to develop. Axons of the cholinergic basal forebrain system are examined, since this is an area that develops axonal swellings in sporadic AD and in TgAPP<sup>Swe</sup> mice. The septal nucleus is part of the basal forebrain cholinergic system and has well-defined axonal termination in the hippocampus, the part of the brain important for learning and memory and severely affected in AD.

## Methods

### Mice and genetic crosses

FAD Swedish APP gene-targeted mice obtained for these studies were originally on the 129/CD-1 genetic background. (Flood *et al.* 2002) We backcrossed these mice onto the C57BL/J6 genetic background for five generations and bred these resulting C57BL/J6 mice for study. All mice included in this study were generated by crossing mice heterozygous for the gene-targeted APP mutations to each other. Mice homozygous for the APP gene-targeted mutations and their age-matched, wild-type littermates were included for study.

J20 transgenic APP mice possessing the FAD Swedish and Indiana mutations on the C57BL/J6 genetic background (Mucke *et al.* 2000) were kindly provided by Dr. Edward Koo. Age-matched, wild-type littermates were used as controls.

### Immunohistochemistry

At various ages, mice were transcardially perfused first with .1M phosphate buffer pH 7.2 (PB) followed by 4% paraformaldehyde in PB (4% PFA). Dissected brains were post-fixed overnight with 4% PFA at 4°C. Coronal sections 50µm thick were cut using a vibrating blade microtome (Leica 1000S), collected in PB, and stored in 30% glycerol cryoprotectant until immunohistochemistry

was performed the next day. For light microscopy every 6<sup>th</sup> section was collected in PB into a serially sampled set representative of the cholinergic basal forebrain and rinsed in PB 3 times for 5 minutes each rinse. Brain slices were then quenched for 1 hour at room temperature with 0.6% hydrogen peroxide and rinsed again in PB. Tissue was blocked and permeabilized for 1 hour at room temperature with 10% serum and .2% Triton X-100 in PB, then incubated in primary antibody ChAT (Invitrogen) diluted 1:100 in the same solution for 72 hours at 4°C. After washing brain sections with PB 6 times for 10 minutes each rinse, tissue was blocked again. Primary antibody signal was enhanced using a biotinylated secondary antibody (Jackson ImmunoResearch) at 1:200 for 1 hour at room temperature, followed by rinsing with PB. Tissue was then incubated with biotin-avidin complexes from the ABC vectastain kit for 1 hour at room temperature, rinsed, and developed with Nova Red (Vector Laboratories). After rinsing with water and mounting onto microscope slides, brain slices were dehydrated in an ethanol series, cleared with xylene for an hour, and mounted with Permount (Fisher). Slides were then coded for blind data collection and analysis using a stereological approach.

Fluorescence microscopy was conducted in a fashion similar to light microscopy. Three serial sections through the hippocampus for each mouse were

collected in PB, rinsed, blocked and permeabilized, then incubated in either primary antibody synaptophysin (Millipore) or ChAT (Invitrogen) at 1:100 overnight at 4°C. After washing brain sections with PB 3 times for 5 minutes each rinse, they were incubated with a fluorophore-conjugated secondary (AlexaFluor) at 1:200 for 1 hour at room temperature. Tissue was mounted with fluorescence-preserving Vectashield media (Vector Laboratories).

### **Stereology**

Brain stereology was performed with an Axioplan Zeiss light microscope associated with a Bioquant Nova Stereology software image analysis system (Bioquant R&M Biometrics, Inc.). In brief, dystrophic cholinergic axon length and number were determined using random, systematically-sampled serial sections of 50µm brain slices. The first slice was selected as the most anterior slice containing the septal nucleus, with every other slice spaced apart by 250µm. Random serial sections were analyzed using the Bioquant system to calculate lengths and numbers of dystrophic axons by tracing non-varicose, dilated axons with widths over 1.5µm in the entire area of each septal nucleus subregion contained in each brain slice. Axonal swelling measurements were conducted by measuring axon and varicosity lengths and widths. Varicosities over 3µm in

diameter were considered axonal swellings (Stokin *et al.* 2005), and the percentage of fibers containing axonal swellings was calculated.

### **Immunofluorescent analyses**

Fluorescent images were collected with an inverted Nikon Bio-Rad Laboratories FV-1000 confocal imaging system and 100x oil immersion objective. Before data collection, confocal acquisition settings to be used for all images were determined to ensure for a linear intensity range below saturation. For synaptophysin imaging 12 images were collected at 6 different sites within the synaptic region of interest, the inner molecular layer of the dentate gyrus, for each brain slice. At each site, 2 images were collected separated by 1 $\mu$ m in the z axis. (Galvan *et al.* 2006) Areas of colocalization for the two images taken at the same site were analyzed using ImageJ software, measuring percent area labeled, particle numbers, and particle sizes. For ChAT imaging, z stacks were collected, consisting of 10 images separated by 1 $\mu$ m. Z stacks were made into maximum projections and analyzed for percent area labeled using ImageJ software. Mean values were obtained for each animal, and animals within the same genotype were pooled for statistical analyses and graphical plotting.

**Western blot analysis**

Dissected mouse brains were collected and immediately frozen in liquid nitrogen. Sample preparation and Western blot technique was performed in a fashion similar to that described in Chapter II.

**Statistics**

Each graph plots genotype means obtained from several animals, and error bars represent the standard error of the mean (SEM). Asterisks indicate statistical significance. For brain stereology and immunofluorescent image analyses, a Mann-Whitney (two sample rank sum) nonparametric statistical test was used at an  $\alpha$  significance of .05.



## Results

### **Expression of humanized APP in backcrossed FAD Swedish gene-targeted mice**

Because Swedish APP gene-targeted mice were backcrossed many generations onto a different genetic background than its original one, we made sure that mice continued to express the humanized APP protein. Western blots were performed on homogenized brain protein from homozygous Swedish APP gene-targeted mice and wild-type mice. Only brain samples from Swedish APP gene-targeted mice showed reactivity to the human-specific APP antibody 6E10. (Figure 3.2) Thus, even after many generations of backcrossing onto a new genetic background, mice still express the gene-targeted mutations.

### **Axonal dystrophy in the septal nucleus of FAD Swedish gene-targeted mice**

Because the FAD Swedish mutations impair APP axonal transport *in vitro*, we wanted to test the hypothesis that the Swedish mutations are sufficient to induce axonal dystrophy *in vivo*. TgAPP<sup>Swe</sup> mice exhibit axonal dystrophy and axonal transport defects, but possess APP mutation as well as overexpression. In this Swedish APP gene-targeted mouse that expresses APP at endogenous levels, ChAT positive cholinergic axons were examined in the various subregions of the basal forebrain septal nucleus. Preliminary observation of these cholinergic

axons did not reveal the presence of axonal swellings, as previously described in TgAPP<sup>Swe</sup> mice and sporadic AD brains. (Stokin *et al.* 2005) Instead, an alternative type of axonal dystrophy was observed that consisted of thick, dilated axons several times the width of normal axons at over 1.5 $\mu$ m in diameter.

Analyses of stereological measurements collected while blinded to genotype revealed a statistically significant increase in cholinergic dilated axons of the septo-hippocampal region of the septal nucleus in gene-targeted APP mice compared to wild-type, age-matched littermates. (Figure 3.3) Both the mean number (WT=5, APP=22.25, n=4,4) and total length (WT=765.84 $\mu$ m, APP=5870.715 $\mu$ m, n=4,4) of dilated axons per mouse brain increased. Similar measurements of dilated axons were taken in the medial septum, which did not indicate a statistically significant increase in mean number (WT=12, APP=17.5, n=4,4) or total length (WT=3280.485 $\mu$ m, APP=3437.46 $\mu$ m, n=4,4) per brain. (Figure 3.4) Similarly, the lateral septum showed no statistically significant increase in mean number (WT=2.25, APP=4.25, n=4,4) or total length (WT=600.51 $\mu$ m, APP=823.605 $\mu$ m, n=4,4) per brain. Thus, gene-targeted Swedish APP mutant mice exhibit cholinergic basal forebrain axonal dystrophy specifically in the septo-hippocampal region, supporting the hypothesis that the Swedish mutations to APP are sufficient to induce axonal dystrophy.

### **Septal nucleus terminal field not affected in FAD Swedish gene-targeted mice**

Because AD brains and mouse models of amyloid pathology exhibit synaptic loss, we wanted to test the hypothesis that the axonal dystrophy observed in Swedish APP gene-targeted mice correlates with synaptic loss in the corresponding terminal field. The septal nucleus sends projections to the hippocampus, and one such terminal field region within the hippocampus is the inner molecular layer of the dentate gyrus. Both cholinergic innervation to this region and presynaptic bouton density were measured using confocal imaging of immunofluorescently-labeled brain slices.

Tests for changes in cholinergic innervation of the inner molecular layer of the dentate gyrus were performed using immunofluorescence for ChAT. Quantitative analysis of high-magnification images indicated no statistically significant change in the percent area labeled with ChAT (WT=24.798%, APP=23.414%, n=4,4), indicating no change in cholinergic innervation of this terminal region. (Figure 3.5) Tests for changes in presynaptic bouton density in the same of the septo-hippocampal terminal field region using quantitative analysis of immunofluorescence for synaptophysin indicated no statistically significant change in the percent of the area labeled with synaptophysin either at

6 months (WT=1.92%, APP=1.53%, n=4,3) or 18 months of age (WT=5.47%, APP=6.19%, n=3,4).

Because the septal nucleus sends projections throughout the hippocampus, we also examined presynaptic bouton density in other hippocampal synaptic regions. Analyses revealed no change in presynaptic bouton density in regions CA1 (WT=5.33%, APP=3.00%, n=3,4) or CA3 (WT=1.61%, APP=3.19%, n=3,3). (Figure 3.6) Thus, axonal dystrophy in the cholinergic basal forebrain septal nucleus of Swedish APP gene-targeted mice does not correspond with loss of cholinergic innervation or presynaptic bouton density in the particular terminal regions examined. Axonal dystrophy that develops in the absence of terminal field changes could indicate that the axonal dystrophy observed represents one of the earliest pathological changes in response to APP Swedish mutation.

#### **No axonal swellings in the NBM of J20 transgenic APP mice**

Transgenic mice that express either FAD Swedish APP under the murine prion protein promoter (TgAPP<sup>Swe</sup>) (Borchelt *et al.* 1997) or FAD Swedish and London APP under the murine Thy1.2 promoter (TgAPP<sup>Swe,Lond</sup>, line 41) (Rockenstein *et al.* 2001) exhibit increased axonal swellings in the cholinergic basal forebrain, specifically in the nucleus basalis of Meynert (NBM). (Stokin *et*

*al.* 2005) We wanted to test if transgenic mice expressing FAD Swedish and Indiana mutant APP under the platelet-derived growth factor  $\beta$  chain promoter (line J20) (Mucke *et al.* 2000) also possess increased axonal swellings in the NBM. ChAT positive cholinergic axons were measured using stereological technique in the NBM of these transgenic mice, and data were compared between transgenic and wild-type, age-matched littermates. Analyses revealed no significant increase in the percent of axons with axonal swellings in the NBM of 3- month (WT=2.85%, n=4 and J20=1.67%, n=4), 6- month (WT=4.67%, n=3 and J20=6.80%, n=5), or 12-month (WT=4.75%, n=4 and J20=4.25%, n=4) old animals. (Figure 3.7) Thus, despite having increased levels of A $\beta$  (Mucke *et al.* 2000), these transgenic APP mice do not possess an increase in cholinergic axonal swellings in the NBM.

## Discussion

In this study we identify axonal dystrophy in a gene-targeted mouse that expresses FAD Swedish mutations to APP, the same mutations found to impair APP axonal transport in Chapter II. The increase in dilated axons, reminiscent of those previously described near amyloid plaques, develops in the absence of other AD-related pathology, such as synaptic loss or amyloid plaque deposition, despite increased  $\beta$ -secretase cleavage and  $A\beta$  generation. This type of axonal dystrophy was specific to the septo-hippocampal region of the septal nucleus, with the lateral and intermediate septal regions not showing such axonal changes. We demonstrate that the FAD Swedish mutations and a humanized  $A\beta$  region to the mouse APP gene are sufficient to induce axonal dystrophy and clarify that overexpression of the mutant protein is not necessary to bring about axonal pathology.

Axonal swellings, as seen in TgAPP<sup>Swe</sup> mice, were not observed in septal nuclei of gene-targeted APP mice. The difference in the type of axonal dystrophies observed in transgenic versus gene-targeted APP mice could be due to APP overexpression in the transgenic mouse versus an endogenous level of expression in the gene-targeted mouse. Another possibility could be that axonal dilation in the absence of amyloid plaque deposition is a phenotype that

precedes axonal swellings. Gene-targeted mice with normal levels of APP expression and no plaque formation might capture early pathological progression, while transgenic mice that overexpress APP and form plaques represent an accelerated pathological process.

There do not seem to be synaptic changes in the inner molecular layer of the dentate gyrus, one projection region of the septo-hippocampal subregion. Quantification of both cholinergic innervation and presynaptic bouton density revealed no changes between wild-type and gene-targeted APP mice. No loss of presynaptic boutons in the dentate gyrus could be due to the mixed population of boutons that reside in that area; not all boutons come from the cholinergic septal nucleus. No loss of cholinergic innervation in the dentate gyrus could be due to cholinergic input from non-septal regions. The lack of presynaptic bouton density and cholinergic innervation changes could also be attributed to the fact that the axonal dilation observed in the septo-hippocampal region of the septal nucleus represents the earliest changes that occur in the pathological process. Terminal fields of dystrophic axons may not yet be affected. As suggested earlier, phenotypes observed in these APP gene-targeted mice with normal APP expression levels likely represent a snapshot of some of the first changes that might occur in the disease process.

Cholinergic axonal dilation develops in these gene-targeted APP mice that undergo increased  $\beta$ -secretase cleavage of APP, but this does not eliminate the possible contribution to the phenotype of A $\beta$  peptides that form after subsequent  $\gamma$ -secretase cleavage. Though numerous studies of transgenic mice correlate increased A $\beta$  generation with axonal dystrophy, A $\beta$ -independent axonopathies can develop as well. TgAPP<sup>Swe</sup> mice possess an increase in axonal swellings, but this phenotype is not enhanced when additional transgenes are expressed that further increase A $\beta$  levels. (Stokin *et al.* 2008) Furthermore, the fact that axonal swellings were not observed in the NBM of J20 FAD Swedish and Indiana APP transgenic mice provides further evidence that an increase in A $\beta$  is not sufficient to induce axonal defects consistent with axonal transport defects. Brains of J20 mice possess approximately equivalent amounts of A $\beta_{42}$  at 12 months of age compared to TgAPP<sup>Swe</sup> mice. (Stokin *et al.* 2005; Galvan *et al.* 2006) Lastly, defects in axonal transport can lead to axonal dystrophy, and research described in Chapter II indicated that impaired axonal transport of APP upon increased  $\beta$ -secretase cleavage likely does not result from increases in A $\beta$ .

We provide evidence that FAD Swedish mutations to APP can not only impair APP axonal transport, but are also sufficient to lead to axonal dystrophy in a gene-targeted mouse. This axonal dystrophy develops in the absence of



amyloid plaques. If FAD Swedish mutations impair APP axonal transport and induce axonal dystrophy, it suggests an interesting possibility that impaired axonal transport of APP caused by aberrant processing could serve as a possible mechanism contributing to the formation of axonal dystrophy seen in AD.

This chapter is currently being prepared for submission and publication of the material. Rodrigues EM and Goldstein LSB. The dissertation author was the primary author and investigator of this paper.

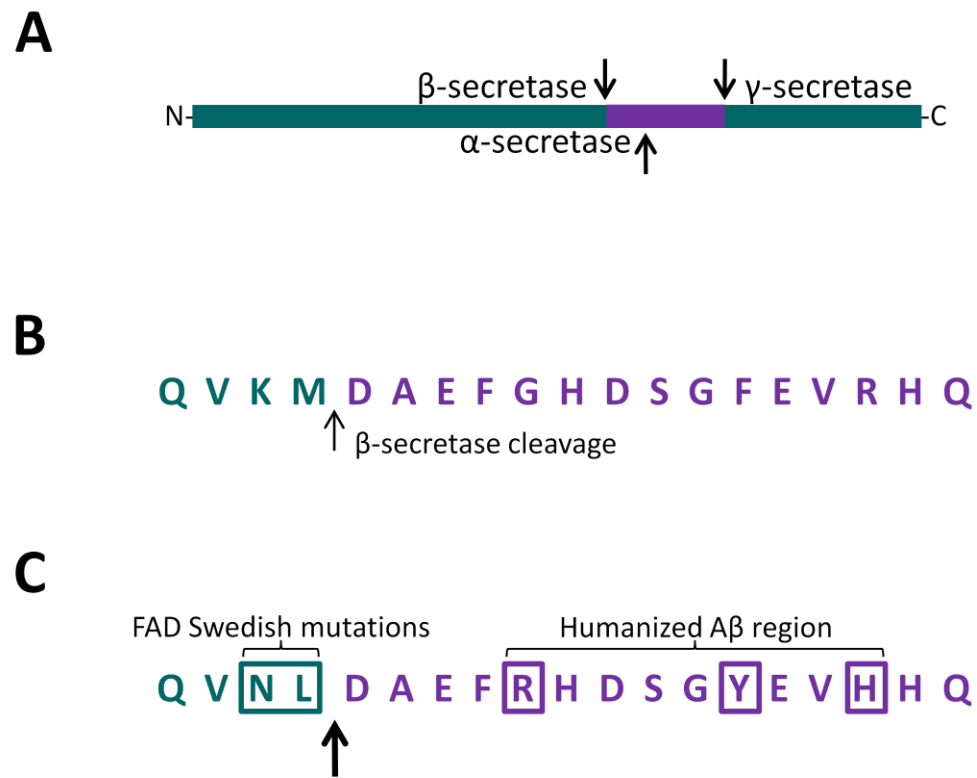


Figure 3.1. Gene-targeted mutations in the mouse APP gene. A) Mouse APP can be cleaved by  $\alpha$ -,  $\beta$ -, and  $\gamma$ -secretases. B) The amino acid sequence flanking the  $\beta$ -secretase cleavage site for the mouse APP protein is shown.  $\beta$ -secretase cleaves at the location indicated by the arrow. C) The APP gene-targeted mouse contains two amino acid changes constituting the FAD Swedish mutations, plus three additional amino acid changes that make the mouse A $\beta$  peptide homologous to the human A $\beta$  peptide.

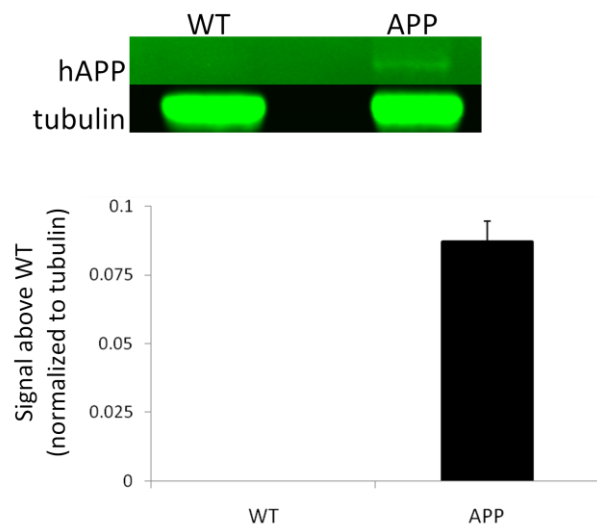


Figure 3.2. Backcrossed gene-targeted mice express humanized APP. In addition to possessing the FAD Swedish mutations in the mouse APP gene, gene-targeted mice also possess mutations to humanize the A $\beta$  region of the mouse APP gene. Brain homogenate from WT and APP mice were loaded onto a Western blot and probed with a human-specific APP antibody. (Top) An example band of 6E10 reactivity is shown for APP mice and absent for WT mice. Tubulin was used as a loading control. (Bottom) Quantification of Western blot analysis is plotted with WT set as 0, indicating the presence of humanized APP for APP gene-targeted mice, but not for WT mice. (n=3)

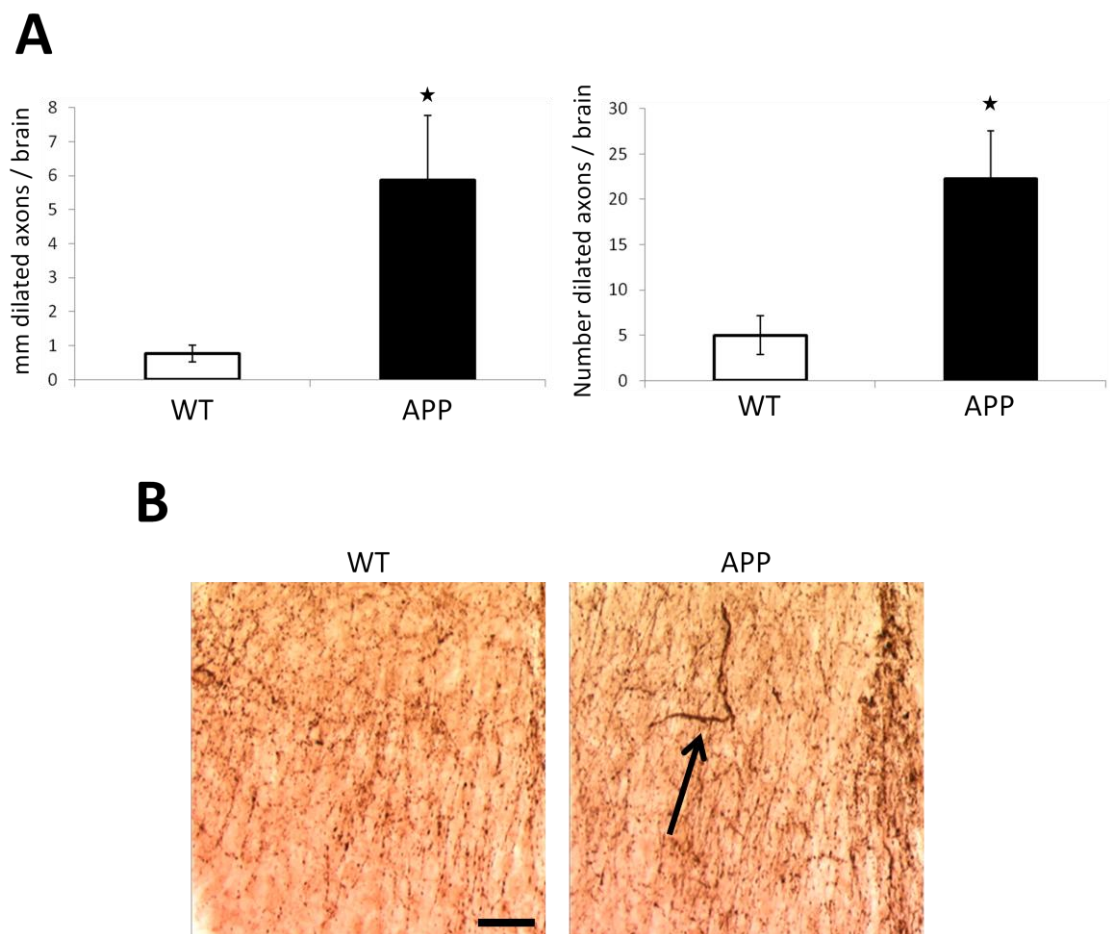


Figure 3.3. Axonal dilation in the septo-hippocampal subregion of the septal nucleus. A) The graph on the left plots the mean total length of cholinergic, dilated axons in the septo-hippocampal subregion of the septal nucleus, while the graph on the right plots the mean total number. APP gene-targeted mice possess significantly increased dilated, cholinergic axons using both measures. (WT n=4, APP n=4) B) Example images of the septo-hippocampal region of ChAT-stained brain slices from WT and APP mice are shown. The black arrow identifies a dilated axon in an APP mouse brain slice.

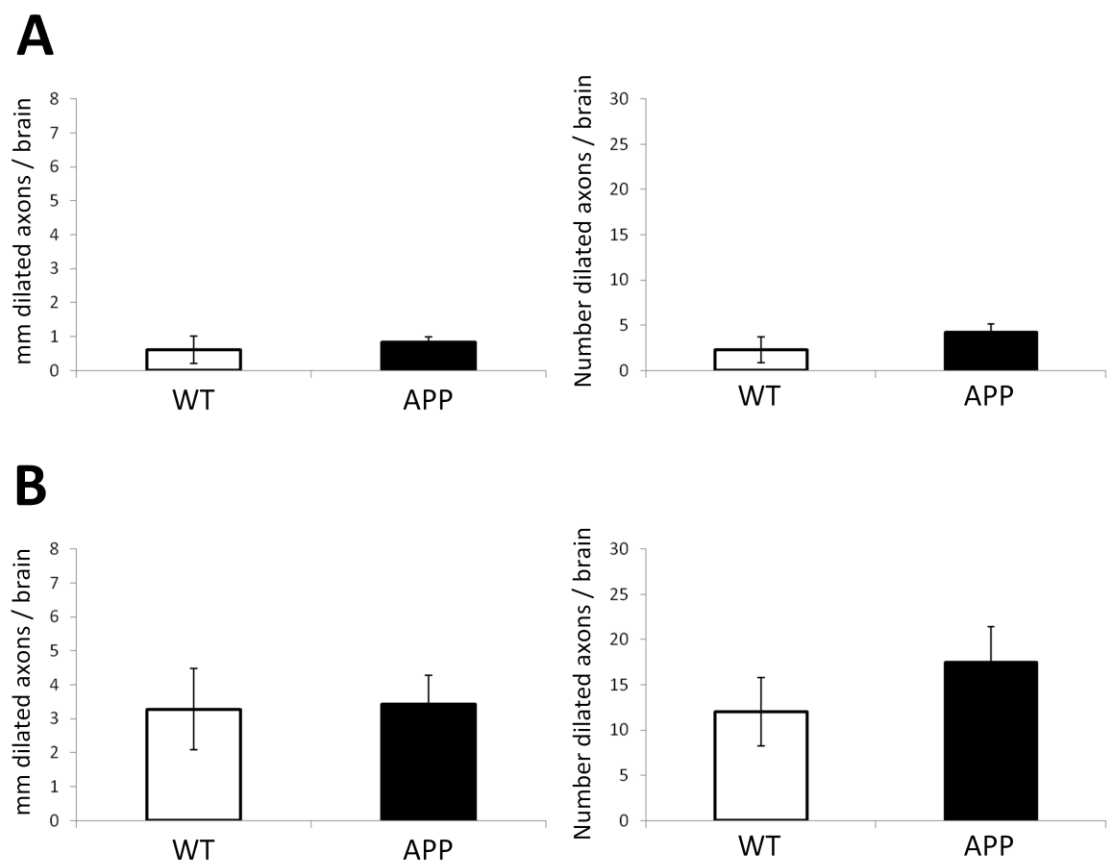


Figure 3.4. No axonal dilation in other subregions of the septal nucleus. The intermediate (A) and medial (B) subregions of the septal nucleus do not possess an increase in cholinergic, dilated axons. The graphs on the left plot the mean total length, while the graphs on the right plot the mean total number. (WT n=4, APP n=4)

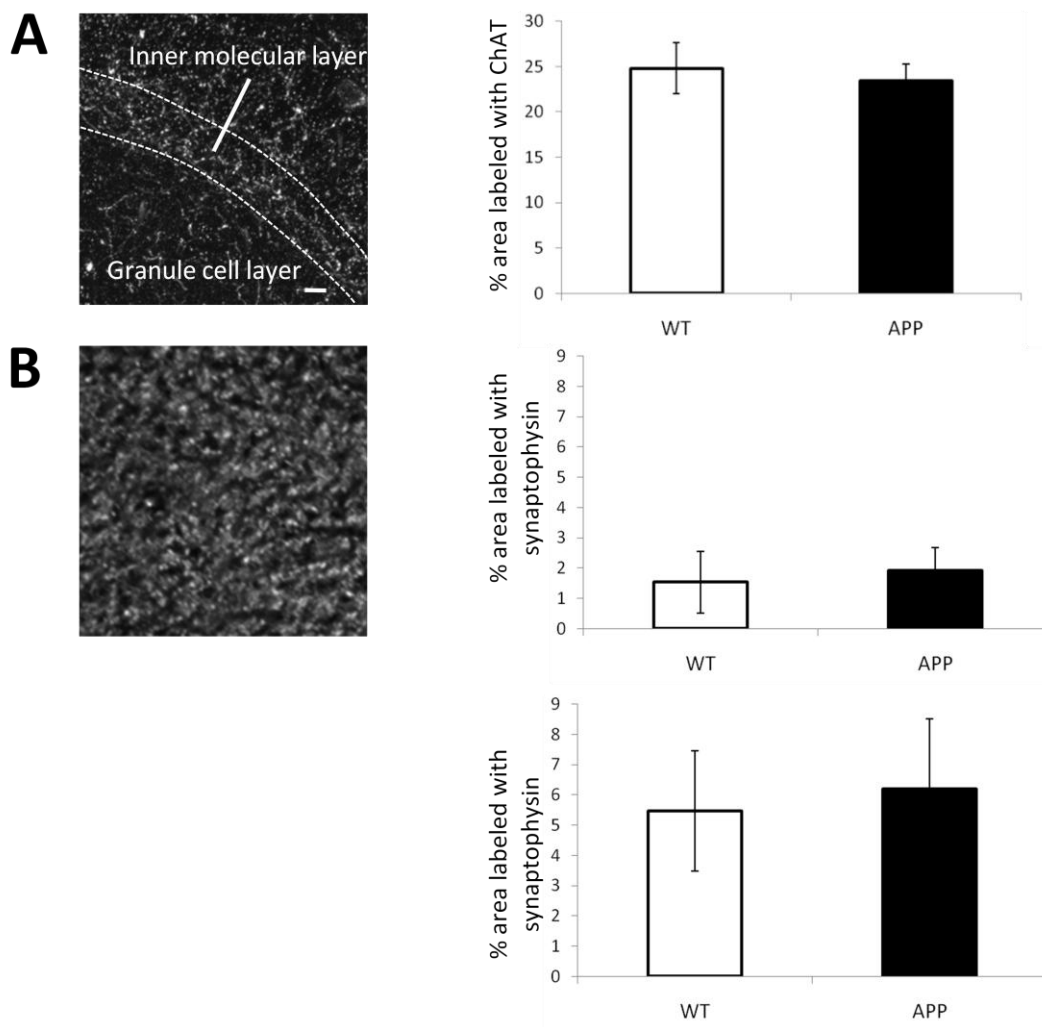


Figure 3.5. No hippocampal terminal field changes in the inner molecular layer of dentate gyrus. A) The left shows an example image of ChAT staining in the inner molecular layer of the dentate gyrus. On the right is a quantification of such images, indicating no change in cholinergic innervation between WT (n=4) and APP (n=4) mice at 18m. B) The left shows an example image of synaptophysin staining in the inner molecular layer of the dentate gyrus. To the right are graphs quantifying such images. There are no significant changes in presynaptic bouton density at either 6m (top) or 18m (bottom).

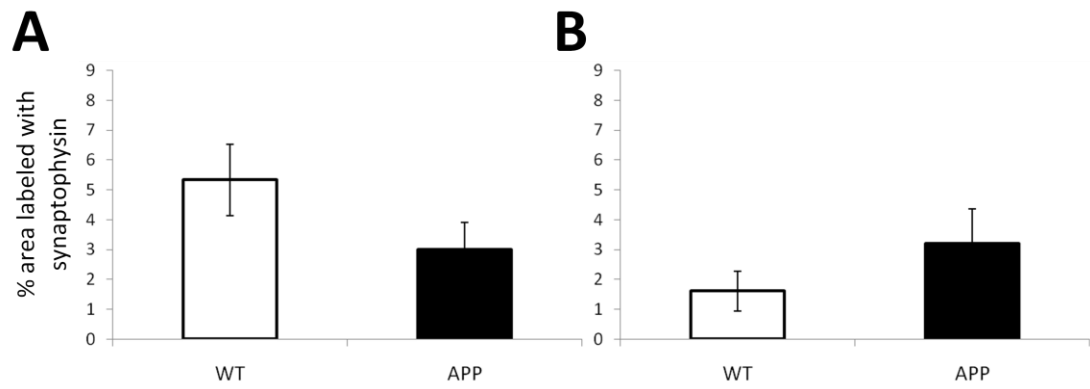


Figure 3.6. No presynaptic bouton density changes in other hippocampal terminal field regions examined. Analyses of regions (A) CA1 at 18m (WT n=3, APP n=4) and (B) CA3 at 24m (WT n=3, APP n=3) do not indicate changes in presynaptic bouton density.

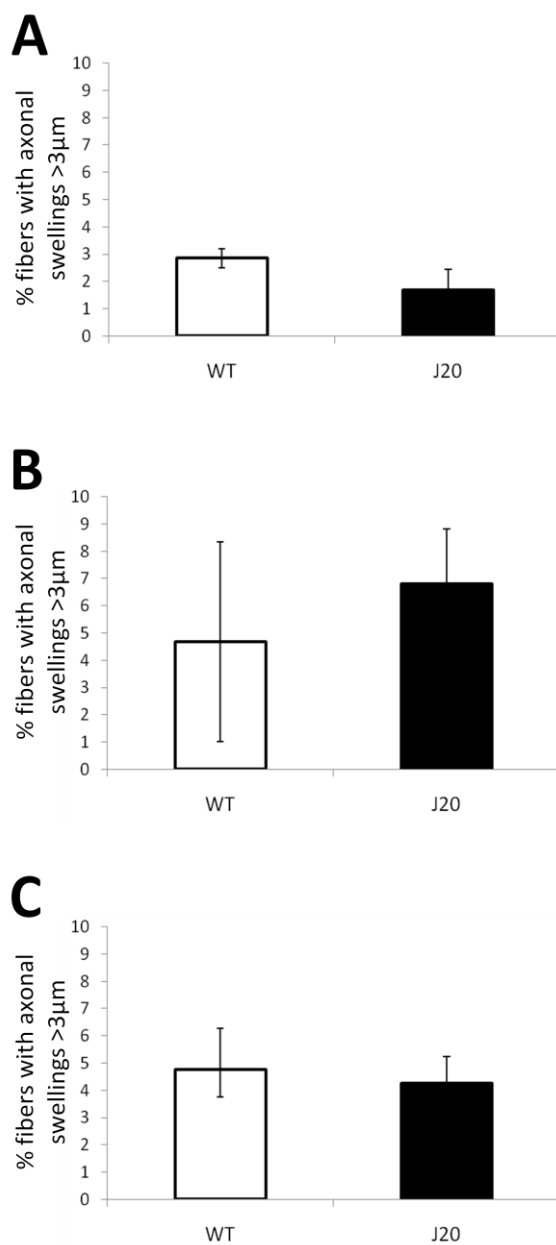


Figure 3.7. No increase in axonal swellings in the NBM of J20 mice. J20 transgenic APP mice do not possess an increase in cholinergic axonal swellings  $>3\mu\text{m}$  in the NBM at (A) 3m (WT n=4, APP n=4), (B) 6m (WT n=3, APP n=5), or (C) 12m (WT n=4, APP n=4).



Chapter IV –  
CONCLUSIONS

AD is a prevalent neurodegenerative disease that involves aberrant APP processing and axonal transport defects. FAD mutations can lead to aberrant APP processing and axonal dystrophy, but it had remained unknown how FAD mutations affect APP axonal transport and if they were sufficient to induce axonal dystrophy. We set out to ask if FAD Swedish mutations to APP can impair APP axonal transport and lead to axonal dystrophy.

We found that mutations at the  $\beta$ -secretase cleavage site of APP can alter APP axonal transport. The FAD Swedish mutations enhancing  $\beta$ -secretase cleavage impair APP anterograde axonal transport, and this effect can be reversed by a  $\beta$ -secretase inhibitor and enhanced by a  $\gamma$ -secretase inhibitor. Conversely, the MV mutation inhibiting  $\beta$ -secretase cleavage has the opposite effect by promoting APP anterograde axonal transport. Thus, not only can  $\beta$ -secretase cleavage of APP regulate its axonal transport, but aberrant amyloidogenic processing can impair APP axonal transport via an apparently  $A\beta$ -independent mechanism.

The FAD Swedish mutations can impair APP axonal transport *in vitro*, but they can also lead to axonal dystrophy *in vivo*, even when the mutant protein is not overexpressed. Transgenic APP mice had previously been shown to possess increased axonal swellings, a type of axonal dystrophy that indicates disrupted

axonal transport, well before the dystrophic neurites associated with amyloid plaques developed. In this study, we show that a gene-targeted mouse expressing FAD Swedish APP with a humanized A $\beta$  region at endogenous levels exhibits increased axonal dystrophy in the cholinergic basal forebrain, despite the fact that plaques never develop.

Because the FAD Swedish mutations to APP can impair APP axonal transport *in vitro* and lead to axonal dystrophy *in vivo*, it suggests an interesting possibility that impaired axonal transport of APP could be one mechanism contributing to the development of axonal dystrophy in AD. APP has been shown to be important for maintaining axonal structure in development and degeneration, so impaired axonal transport of APP could affect axonal health. (Nikolaev *et al* 2009; Qiu *et al.* 1995; Muller *et al.* 1994) Normal delivery, function, and signaling of APP and other factors co-transported with it in cargo vesicles would be disrupted with impaired APP axonal transport. (Abe *et al.* 2009) Additionally, defects in APP axonal transport could cause obstructions in the axon that lead to pathological accumulations of vesicles and organelles that block axonal transport in general and harm axonal health.

Disruption in APP axonal transport upon aberrant APP processing appears to be A $\beta$ -independent and could represent one of the earliest defects

leading to other AD-related pathology. Axonal transport defects can contribute to amyloid and tau pathology, both hallmark characteristics of AD. TgAPP<sup>Swe</sup> mice have increased axonal swellings, A $\beta$  levels, and amyloid plaque deposition upon an ordinarily benign reduction in KLC1. (Stokin *et al.* 2005) Mice lacking KLC1 develop axonal swellings, activation of stress kinases, and abnormal tau hyperphosphorylation and accumulation. (Falzone *et al.* 2009) Thus, defects in axonal transport can serve as a common mechanism for the development of AD-related amyloid and tau pathology. Impaired axonal transport of APP resulting from aberrant processing could potentially further contribute to increased amyloidogenesis and abnormal tau phosphorylation. Amyloidogenesis and abnormal tau phosphorylation would eventually further disrupt general axonal transport mechanisms. This possible cascade of events would present a vicious cycle of cellular demise progressing towards the pathology characterizing AD.

## REFERENCES

Abe N, Almenar-Queralt A, Lillo C, Shen Z, Lozach J, Briggs SP, Williams DS, Goldstein LS, Cavalli V (2009) Sunday driver interacts with two distinct classes of axonal organelles. *J Biol Chem* 284:34628-34639.

Abramov E, Dolev I, Fogel H, Ciccotosto GD, Ruff E, Slutsky I (2009) Amyloid-beta as a positive endogenous regulator of release probability at hippocampal synapses. *Nat Neurosci* 12:1567-1576.

Amaratunga A, Morin PJ, Kosik KS, Fine RE (1993) Inhibition of kinesin synthesis and rapid anterograde axonal transport in vivo by an antisense oligonucleotide. *J Biol Chem* 268:17427-17430.

Amaratunga A, Fine RE (1995) Generation of amyloidogenic C-terminal fragments during rapid axonal transport in vivo of beta-amyloid precursor protein in the optic nerve. *J Biol Chem* 270:17268-17272.

Amaratunga A, Leeman SE, Kosik KS, Fine RE (1995) Inhibition of kinesin synthesis in vivo inhibits the rapid transport of representative proteins for three transport vesicle classes into the axon. *J Neurochem* 64:2374-2376.

Borchelt DR, Ratovitski T, van Lare J, Lee MK, Gonzales V, Jenkins NA, Copeland NG, Price DL, Sisodia SS (1997) Accelerated amyloid deposition in the brains of transgenic mice coexpressing mutant presenilin 1 and amyloid precursor proteins. *Neuron* 19:939-945.

Buxbaum JD, Thinakaran G, Koliatsos V, O'Callahan J, Slunt HH, Price DL, Sisodia SS (1998) Alzheimer amyloid protein precursor in the rat hippocampus: transport and processing through the perforant path. *J Neurosci* 18:9629-9637.

Cai D, Leem JY, Greenfield JP, Wang P, Kim BS, Wang R, Lopes KO, Kim SH, Zheng H, Greengard P, Sisodia SS, Thinakaran G, Xu H (2003) Presenilin-1 regulates intracellular trafficking and cell surface delivery of beta-amyloid precursor protein. *J Biol Chem* 278:3446-3454.

Calabrese B, Shaked GM, Tabarean IV, Braga J, Koo EH, Halpain S (2007) Rapid, concurrent alterations in pre- and postsynaptic structure induced by naturally-secreted amyloid-beta protein. *Mol Cell Neurosci* 35:183-193.

Cavalli V, Kujala P, Klumperman J, Goldstein LS (2005) Sunday Driver links axonal transport to damage signaling. *J Cell Biol* 168:775-787.

Chapman PF, White GL, Jones MW, Cooper-Blacketer D, Marshall VJ, Irizarry M, Younkin L, Good MA, Bliss TV, Hyman BT, Younkin SG, Hsiao KK (1999) Impaired synaptic plasticity and learning in aged amyloid precursor protein transgenic mice. *Nat Neurosci* 2:271-276.

Cirrito JR, Yamada KA, Finn MB, Sloviter RS, Bales KR, May PC, Schoepp DD, Paul SM, Mennerick S, Holtzman DM (2005) Synaptic activity regulates interstitial fluid amyloid-beta levels in vivo. *Neuron* 48:913-922.

Crowther RA, Goedert M (2000) Abnormal tau-containing filaments in neurodegenerative diseases. *J Struct Biol* 130:271-279.

Dai J, Buijs RM, Kamphorst W, Swaab DF (2002) Impaired axonal transport of cortical neurons in Alzheimer's disease is associated with neuropathological changes. *Brain Res* 948:138-144.

Decker H, Lo KY, Unger SM, Ferreira ST, Silverman MA (2010) Amyloid-beta peptide oligomers disrupt axonal transport through an NMDA receptor-dependent mechanism that is mediated by glycogen synthase kinase 3beta in primary cultured hippocampal neurons. *J Neurosci* 30:9166-9171.

Dhaenens CM, Van Brussel E, Schraen-Maschke S, Pasquier F, Delacourte A, Sablonniere B (2004) Association study of three polymorphisms of kinesin light-chain 1 gene with Alzheimer's disease. *Neurosci Lett* 368:290-292.

Falzone TL, Stokin GB, Lillo C, Rodrigues EM, Westerman EL, Williams DS, Goldstein LS (2009) Axonal stress kinase activation and tau misbehavior induced by kinesin-1 transport defects. *J Neurosci* 29:5758-5767.

Flood DG, Reaume AG, Dorfman KS, Lin YG, Lang DM, Trusko SP, Savage MJ, Annaert WG, De Strooper B, Siman R, Scott RW (2002) FAD mutant PS-1 gene-targeted mice: increased A beta 42 and A beta deposition without APP overproduction. *Neurobiol Aging* 23:335-348.

Friedhoff P, von Bergen M, Mandelkow EM, Mandelkow E (2000) Structure of tau protein and assembly into paired helical filaments. *Biochim Biophys Acta* 1502:122-132.

Galvan V, Gorostiza OF, Banwait S, Ataie M, Logvinova AV, Sitaraman S, Carlson E, Sagi SA, Chevallier N, Jin K, Greenberg DA, Bredesen DE (2006) Reversal of Alzheimer's-like pathology and behavior in human APP transgenic mice by mutation of Asp664. *Proc Natl Acad Sci U S A* 103:7130-7135.

Goldstein LS (2003) Do disorders of movement cause movement disorders and dementia? *Neuron* 40:415-425.

Gralle M, Botelho MG, Wouters FS (2009) Neuroprotective secreted amyloid precursor protein acts by disrupting amyloid precursor protein dimers. *J Biol Chem* 284:15016-15025.

Gunawardena S, Goldstein LS (2001) Disruption of axonal transport and neuronal viability by amyloid precursor protein mutations in *Drosophila*. *Neuron* 32:389-401.

Hiruma H, Katakura T, Takahashi S, Ichikawa T, Kawakami T (2003) Glutamate and amyloid beta-protein rapidly inhibit fast axonal transport in cultured rat hippocampal neurons by different mechanisms. *J Neurosci* 23:8967-8977.

Hurd DD, Saxton WM (1996) Kinesin mutations cause motor neuron disease phenotypes by disrupting fast axonal transport in *Drosophila*. *Genetics* 144:1075-1085.

Jiang Y, Mullaney KA, Peterhoff CM, Che S, Schmidt SD, Boyer-Boiteau A, Ginsberg SD, Cataldo AM, Mathews PM, Nixon RA (2010) Alzheimer's-related endosome dysfunction in Down syndrome is A $\beta$ -independent but requires APP and is reversed by BACE-1 inhibition. *Proc Natl Acad Sci U S A* 107:1630-1635.

Kaether C, Skehel P, Dotti CG (2000) Axonal membrane proteins are transported in distinct carriers: a two-color video microscopy study in cultured hippocampal neurons. *Mol Biol Cell* 11:1213-1224.



Kamal A, Stokin GB, Yang Z, Xia CH, Goldstein LS (2000) Axonal transport of amyloid precursor protein is mediated by direct binding to the kinesin light chain subunit of kinesin-I. *Neuron* 28:449-459.

Kamal A, Almenar-Queralt A, LeBlanc JF, Roberts EA, Goldstein LS (2001) Kinesin-mediated axonal transport of a membrane compartment containing beta-secretase and presenilin-1 requires APP. *Nature* 414:643-648.

Kawarabayashi T, Shoji M, Yamaguchi H, Tanaka M, Harigaya Y, Ishiguro K, Hirai S (1993) Amyloid beta protein precursor accumulates in swollen neurites throughout rat brain with aging. *Neurosci Lett* 153:73-76.

Kim SH, Leem JY, Lah JJ, Slunt HH, Levey AI, Thinakaran G, Sisodia SS (2001) Multiple effects of aspartate mutant presenilin 1 on the processing and trafficking of amyloid precursor protein. *J Biol Chem* 276:43343-43350.

Koo EH, Sisodia SS, Archer DR, Martin LJ, Weidemann A, Beyreuther K, Fischer P, Masters CL, Price DL (1990) Precursor of amyloid protein in Alzheimer disease undergoes fast anterograde axonal transport. *Proc Natl Acad Sci U S A* 87:1561-1565.

LaMonte BH, Wallace KE, Holloway BA, Shelly SS, Ascano J, Tokito M, Van Winkle T, Howland DS, Holzbaur EL (2002) Disruption of dynein/dynactin inhibits axonal transport in motor neurons causing late-onset progressive degeneration. *Neuron* 34:715-727.

Lazarov O, Lee M, Peterson DA, Sisodia SS (2002) Evidence that synaptically released beta-amyloid accumulates as extracellular deposits in the hippocampus of transgenic mice. *J Neurosci* 22:9785-9793.

Leem JY, Saura CA, Pietrzik C, Christianson J, Wanamaker C, King LT, Veselits ML, Tomita T, Gasparini L, Iwatsubo T, Xu H, Green WN, Koo EH, Thinakaran G (2002) A role for presenilin 1 in regulating the delivery of amyloid precursor protein to the cell surface. *Neurobiol Dis* 11:64-82.

Masliah E, Iimoto DS, Saitoh T, Hansen LA, Terry RD (1990) Increased immunoreactivity of brain spectrin in Alzheimer disease: a marker for synapse loss? *Brain Res* 531:36-44.

- Morin PJ, Abraham CR, Amaratunga A, Johnson RJ, Huber G, Sandell JH, Fine RE (1993) Amyloid precursor protein is synthesized by retinal ganglion cells, rapidly transported to the optic nerve plasma membrane and nerve terminals, and metabolized. *J Neurochem* 61:464-473.
- Moya KL, Confaloni AM, Allinquant B (1994) In vivo neuronal synthesis and axonal transport of Kunitz protease inhibitor (KPI)-containing forms of the amyloid precursor protein. *J Neurochem* 63:1971-1974.
- Moya KL, Benowitz LI, Schneider GE, Allinquant B (1994) The amyloid precursor protein is developmentally regulated and correlated with synaptogenesis. *Dev Biol* 161:597-603.
- Mucke L, Masliah E, Yu GQ, Mallory M, Rockenstein EM, Tatsuno G, Hu K, Kholodenko D, Johnson-Wood K, McConlogue L (2000) High-level neuronal expression of abeta 1-42 in wild-type human amyloid protein precursor transgenic mice: synaptotoxicity without plaque formation. *J Neurosci* 20:4050-4058.
- Muller U, Cristina N, Li ZW, Wolfer DP, Lipp HP, Rulicke T, Brandner S, Aguzzi A, Weissmann C (1994) Behavioral and anatomical deficits in mice homozygous for a modified beta-amyloid precursor protein gene. *Cell* 79:755-765.
- Muresan V, Varvel NH, Lamb BT, Muresan Z (2009) The cleavage products of amyloid-beta precursor protein are sorted to distinct carrier vesicles that are independently transported within neurites. *J Neurosci* 29:3565-3578.
- Nikolaev A, McLaughlin T, O'Leary DD, Tessier-Lavigne M (2009) APP binds DR6 to trigger axon pruning and neuron death via distinct caspases. *Nature* 457:981-989.
- Pigino G, Morfini G, Pelsman A, Mattson MP, Brady ST, Busciglio J (2003) Alzheimer's presenilin 1 mutations impair kinesin-based axonal transport. *J Neurosci* 23:4499-4508.
- Pigino G, Morfini G, Atagi Y, Deshpande A, Yu C, Jungbauer L, LaDu M, Busciglio J, Brady S (2009) Disruption of fast axonal transport is a pathogenic

mechanism for intraneuronal amyloid beta. *Proc Natl Acad Sci U S A* 106:5907-5912.

Puls I, Jonnakuty C, LaMonte BH, Holzbaur EL, Tokito M, Mann E, Floeter MK, Bidus K, Drayna D, Oh SJ, Brown RH, Jr., Ludlow CL, Fischbeck KH (2003) Mutant dynactin in motor neuron disease. *Nat Genet* 33:455-456.

Qiu WQ, Ferreira A, Miller C, Koo EH, Selkoe DJ (1995) Cell-surface beta-amyloid precursor protein stimulates neurite outgrowth of hippocampal neurons in an isoform-dependent manner. *J Neurosci* 15:2157-2167.

Reaume AG, Howland DS, Trusko SP, Savage MJ, Lang DM, Greenberg BD, Siman R, Scott RW (1996) Enhanced amyloidogenic processing of the beta-amyloid precursor protein in gene-targeted mice bearing the Swedish familial Alzheimer's disease mutations and a "humanized" A $\beta$  sequence. *J Biol Chem* 271:23380-23388.

Reid E, Kloos M, Ashley-Koch A, Hughes L, Bevan S, Svenson IK, Graham FL, Gaskell PC, Dearlove A, Pericak-Vance MA, Rubinsztein DC, Marchuk DA (2002) A kinesin heavy chain (KIF5A) mutation in hereditary spastic paraplegia (SPG10). *Am J Hum Genet* 71:1189-1194.

Rockenstein E, Mallory M, Mante M, Sisk A, Masliah E (2001) Early formation of mature amyloid-beta protein deposits in a mutant APP transgenic model depends on levels of A $\beta$ (1-42). *J Neurosci Res* 66:573-582.

Roher AE, Weiss N, Kokjohn TA, Kuo YM, Kalback W, Anthony J, Watson D, Luehrs DC, Sue L, Walker D, Emmerling M, Goux W, Beach T (2002) Increased A $\beta$  peptides and reduced cholesterol and myelin proteins characterize white matter degeneration in Alzheimer's disease. *Biochemistry* 41:11080-11090.

Roy S, Zhang B, Lee VM, Trojanowski JQ (2005) Axonal transport defects: a common theme in neurodegenerative diseases. *Acta Neuropathol* 109:5-13.

Rui Y, Tiwari P, Xie Z, Zheng JQ (2006) Acute impairment of mitochondrial trafficking by beta-amyloid peptides in hippocampal neurons. *J Neurosci* 26:10480-10487.

Salehi A, Delcroix JD, Belichenko PV, Zhan K, Wu C, Valletta JS, Takimoto-Kimura R, Kleschevnikov AM, Sambamurti K, Chung PP, Xia W, Villar A, Campbell WA, Kulnane LS, Nixon RA, Lamb BT, Epstein CJ, Stokin GB, Goldstein LS, Mobley WC (2006) Increased App expression in a mouse model of Down's syndrome disrupts NGF transport and causes cholinergic neuron degeneration. *Neuron* 51:29-42.

Scheuermann S, Hamsch B, Hesse L, Stumm J, Schmidt C, Beher D, Bayer TA, Beyreuther K, Multhaup G (2001) Homodimerization of amyloid precursor protein and its implication in the amyloidogenic pathway of Alzheimer's disease. *J Biol Chem* 276:33923-33929.

Scheuner D, Eckman C, Jensen M, Song X, Citron M, Suzuki N, Bird TD, Hardy J, Hutton M, Kukull W, Larson E, Levy-Lahad E, Viitanen M, Peskind E, Poorkaj P, Schellenberg G, Tanzi R, Wasco W, Lannfelt L, Selkoe D, Younkin S (1996) Secreted amyloid beta-protein similar to that in the senile plaques of Alzheimer's disease is increased in vivo by the presenilin 1 and 2 and APP mutations linked to familial Alzheimer's disease. *Nat Med* 2:864-870.

Sheng JG, Price DL, Koliatsos VE (2002) Disruption of corticocortical connections ameliorates amyloid burden in terminal fields in a transgenic model of A $\beta$  amyloidosis. *J Neurosci* 22:9794-9799.

Sisodia SS, Koo EH, Hoffman PN, Perry G, Price DL (1993) Identification and transport of full-length amyloid precursor proteins in rat peripheral nervous system. *J Neurosci* 13:3136-3142.

Smith DH, Chen XH, Iwata A, Graham DI (2003) Amyloid beta accumulation in axons after traumatic brain injury in humans. *J Neurosurg* 98:1072-1077.

Soba P, Eggert S, Wagner K, Zentgraf H, Siehl K, Kreger S, Lower A, Langer A, Merdes G, Paro R, Masters CL, Muller U, Kins S, Beyreuther K (2005) Homo- and heterodimerization of APP family members promotes intercellular adhesion. *Embo J* 24:3624-3634.

Stokin GB, Lillo C, Falzone TL, Brusch RG, Rockenstein E, Mount SL, Raman R, Davies P, Masliah E, Williams DS, Goldstein LS (2005) Axonopathy and transport deficits early in the pathogenesis of Alzheimer's disease. *Science* 307:1282-1288.

Suzuki N, Cheung TT, Cai XD, Odaka A, Otvos L, Jr., Eckman C, Golde TE, Younkin SG (1994) An increased percentage of long amyloid beta protein secreted by familial amyloid beta protein precursor (beta APP717) mutants. *Science* 264:1336-1340.

Tampellini D, Rahman N, Gallo EF, Huang Z, Dumont M, Capetillo-Zarate E, Ma T, Zheng R, Lu B, Nanus DM, Lin MT, Gouras GK (2009) Synaptic activity reduces intraneuronal A $\beta$ , promotes APP transport to synapses, and protects against A $\beta$ -related synaptic alterations. *J Neurosci* 29:9704-9713.

Tokuda T, Kametani F, Tanaka K, Sahara N, Ikeda S, Yanagisawa N (1996) Amyloid beta protein and its 3-kDa fragment are present in the axoplasm fraction of the white matter in human brain. *Biochem Biophys Res Commun* 223:165-169.

Torroja L, Chu H, Kotovsky I, White K (1999) Neuronal overexpression of APPL, the *Drosophila* homologue of the amyloid precursor protein (APP), disrupts axonal transport. *Curr Biol* 9:489-492.

Uchihara T, Kondo H, Akiyama H, Ikeda K (1995) White matter amyloid in Alzheimer's disease brain. *Acta Neuropathol* 90:51-56.

Vossel KA, Zhang K, Brodbeck J, Daub AC, Sharma P, Finkbeiner S, Cui B, Mucke L (2010) Tau Reduction Prevents A $\beta$ -Induced Defects in Axonal Transport. *Science*.

Wang Y, Ha Y (2004) The X-ray structure of an antiparallel dimer of the human amyloid precursor protein E2 domain. *Mol Cell* 15:343-353.

Wang P, Yang G, Mosier DR, Chang P, Zaidi T, Gong YD, Zhao NM, Dominguez B, Lee KF, Gan WB, Zheng H (2005) Defective neuromuscular synapses in mice lacking amyloid precursor protein (APP) and APP-Like protein 2. *J Neurosci* 25:1219-1225.

Wei W, Nguyen LN, Kessels HW, Hagiwara H, Sisodia S, Malinow R (2010) Amyloid beta from axons and dendrites reduces local spine number and plasticity. *Nat Neurosci* 13:190-196.

Wirhth O, Multhaup G, Czech C, Feldmann N, Blanchard V, Tremp G, Beyreuther K, Pradier L, Bayer TA (2002) Intraneuronal APP/A beta trafficking and plaque formation in beta-amyloid precursor protein and presenilin-1 transgenic mice. *Brain Pathol* 12:275-286.

Wisniewski HM, Narang HK, Terry RD (1976) Neurofibrillary tangles of paired helical filaments. *J Neurol Sci* 27:173-181.

Zhao C, Takita J, Tanaka Y, Setou M, Nakagawa T, Takeda S, Yang HW, Terada S, Nakata T, Takei Y, Saito M, Tsuji S, Hayashi Y, Hirokawa N (2001) Charcot-Marie-Tooth disease type 2A caused by mutation in a microtubule motor KIF1Bbeta. *Cell* 105:587-597.